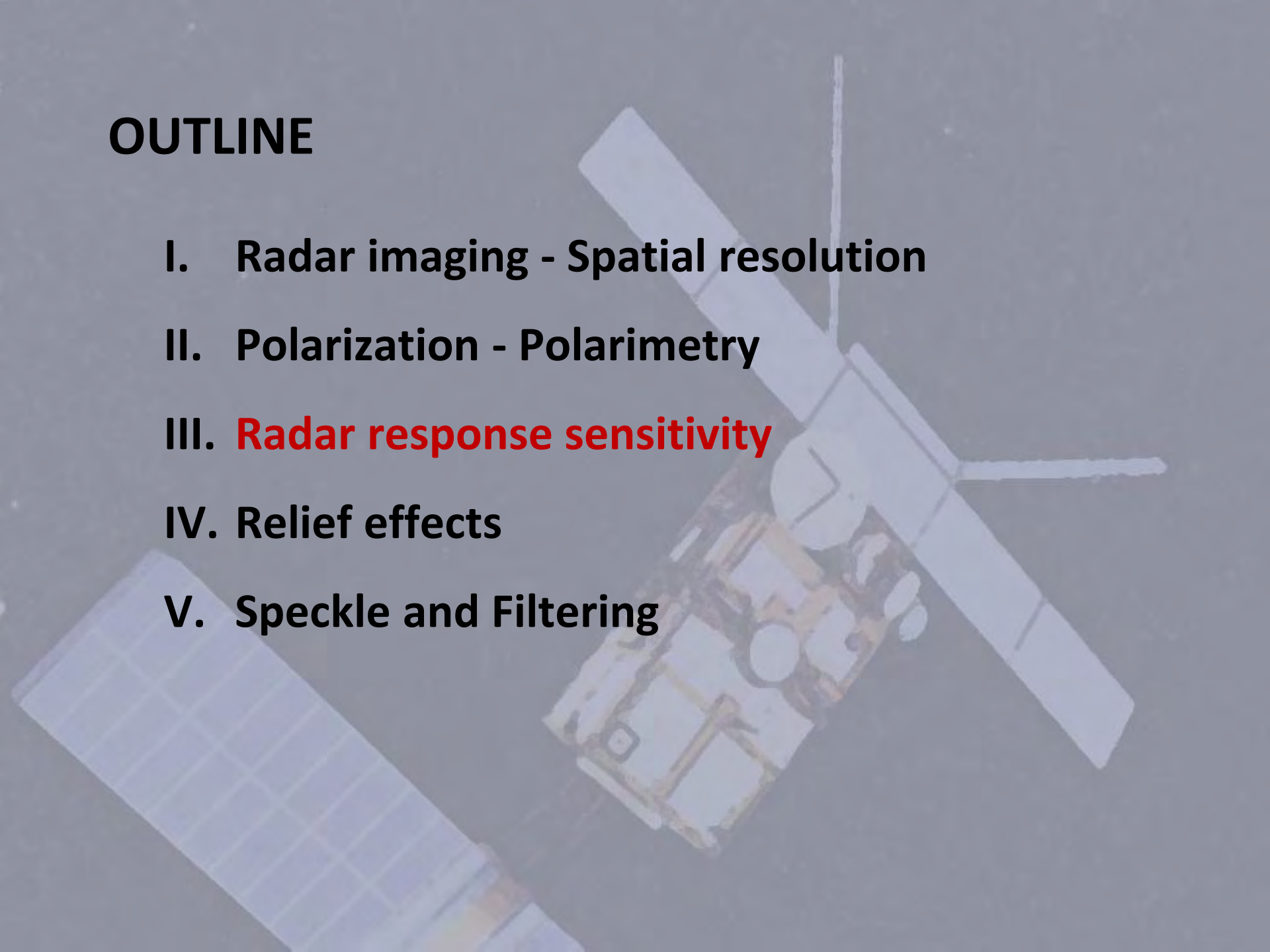


OUTLINE

- I. Radar imaging - Spatial resolution
- II. Polarization - Polarimetry
- III. **Radar response sensitivity**
- IV. Relief effects
- V. Speckle and Filtering



The radar equation

Transmitted power:

$$P_i = \frac{P_e G_e}{4\pi} d\Omega \quad (W)$$

Receiving irradiance at distance R:

$$E_i = \frac{P_e G_e}{4\pi R^2} \quad (W/m^2)$$

Intercepted power from the target (W):

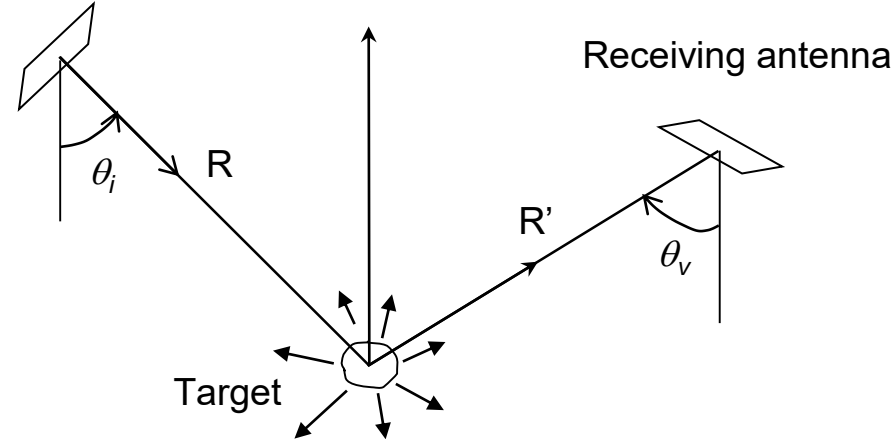
$$P_s = \frac{P_e G_e}{4\pi R^2} \text{RCS} \quad \text{Radar Cross Section (m}^2\text{)}$$

Intensity emitted from the target (isotrope):

$$I = \frac{P_s}{4\pi} = \frac{P_e G_e}{4\pi R^2} \frac{\text{RCS}}{4\pi} \quad (W/sr)$$

Power received by surface dS at distance R': $P_r = I d\Omega = I \frac{dS}{R'^2} = \frac{P_e G_e}{4\pi R^2} \frac{\text{RCS}}{4\pi R'^2} dS \quad (W)$

Transmitting antenna



The radar equation

Power received by dS at distance R'

$$P_r = \frac{P_e G_e}{4\pi R^2} \frac{RCS}{4\pi R'^2} dS \quad (W)$$

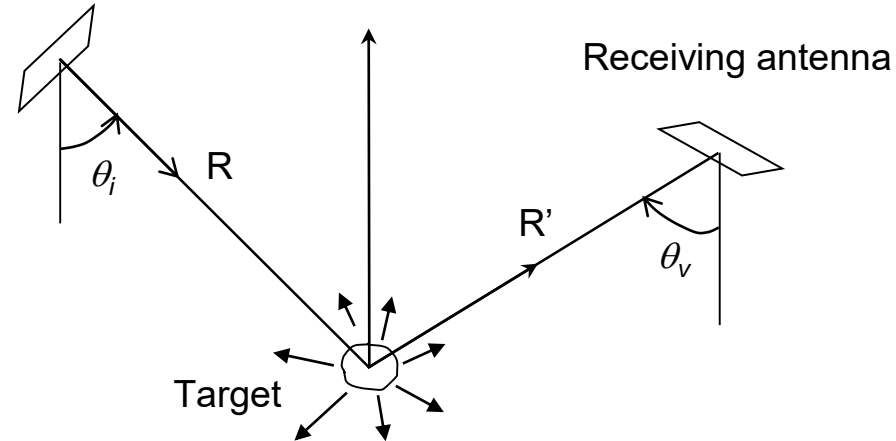
Received irradiance at distance R'

$$E_r = \frac{P_e G_e}{4\pi R^2} \frac{RCS}{4\pi R'^2} \quad (W/m^2)$$

Power received by the antenna: $P_r = E_r dA = E_r \frac{G_r \lambda^2}{4\pi} = \frac{P_e G_e}{4\pi R^2} \frac{RCS}{4\pi R'^2} \frac{G_r \lambda^2}{4\pi}$

(W)

Transmitting antenna



The radar equation

Power received by the antenna:

$$dP_r = \frac{P_e G_e}{4\pi R^2} \frac{\text{RCS}}{4\pi} \frac{G_r \lambda^2}{4\pi R^2} \quad (W)$$

↖ Radar Cross Section (m²)

Case of expanse surfaces:

Radar Backscattering Coefficient:

$$\sigma^0 = \frac{\text{RCS}}{d\Sigma} \quad (m^2/m^2)$$

➔ Analogous to the reflectance in Optical domain

$$dP_r = \frac{P_e G_e}{4\pi R^2} \frac{\sigma^0 d\Sigma}{4\pi} \frac{G_r \lambda^2}{4\pi R^2}$$

$$\sigma^0 = \frac{(4\pi)^3}{\lambda^2} \frac{\langle P_r \rangle}{P_e} \frac{R^4}{\iint_{\text{Surf. obs.}} G_e G_r d\Sigma}$$

σ^0 high dynamic

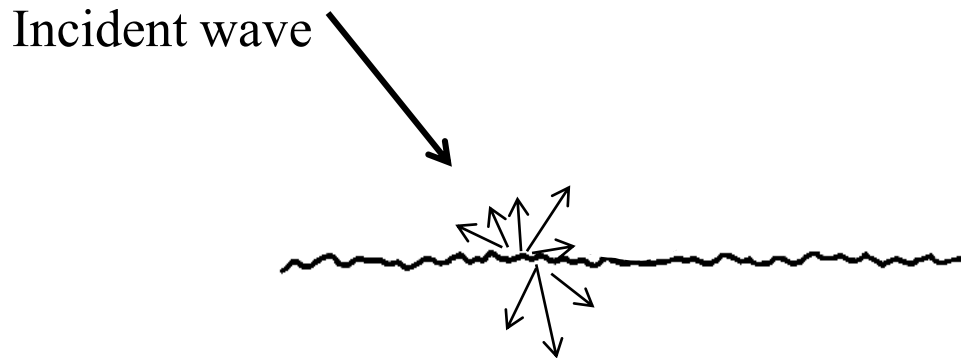
==> dB units (log. scale)

$$\sigma_{dB}^0 = 10 \cdot \log_{10} \left(\sigma_{Nat}^0 \right)$$

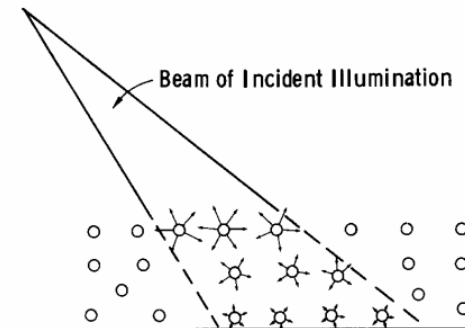
Radar images interpretation rules

2 cases of figure:

Surface scattering (interaction occurs at the interface between both media)



Volume scattering (interaction with multiple elements = scatterers)



Radar response sensitivity

bare soils or water surfaces

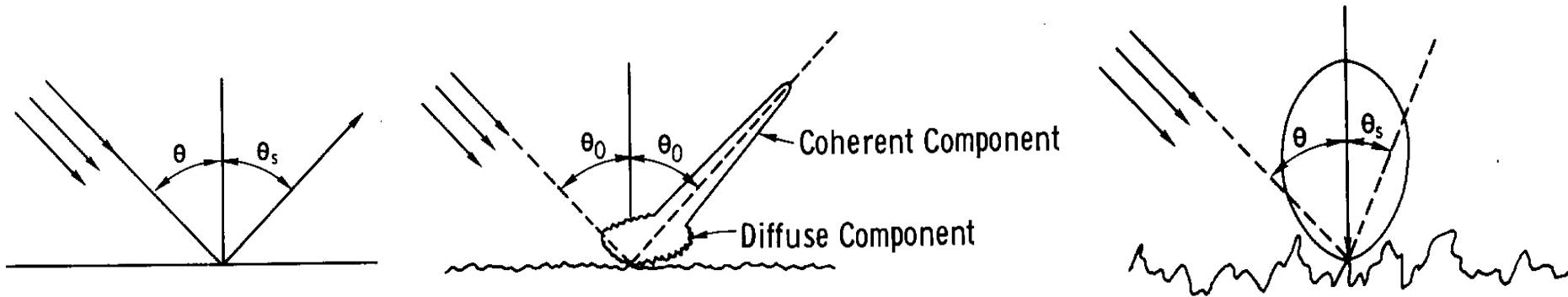
Surface Scattering

Radar images interpretation rules

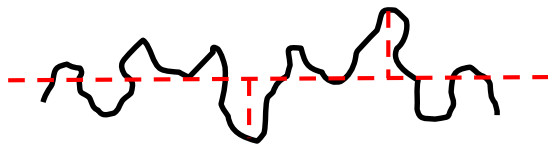
Surface scattering

Soil: homogeneous medium ==> scattering at the interface

Influence of roughness



Surface roughness is referred to the radar wavelength



σ : rms height

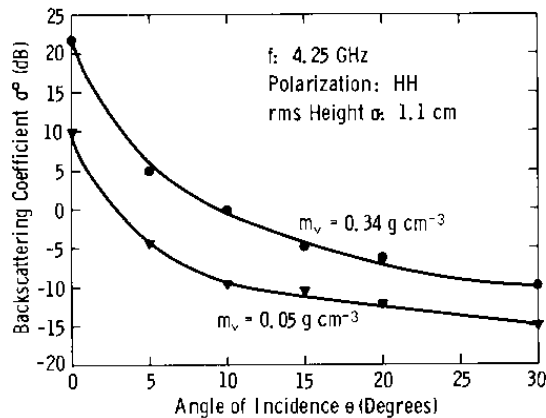
$$\sigma < \frac{\lambda}{8 \cos \theta} \quad ==> \text{smooth surface}$$

ERS ($\lambda = 5 \text{ cm}$, $\theta = 23^\circ$): $s > 2 \cdot 10^{-2}$: every soil is rough!

Radar images interpretation rules

Surface scattering

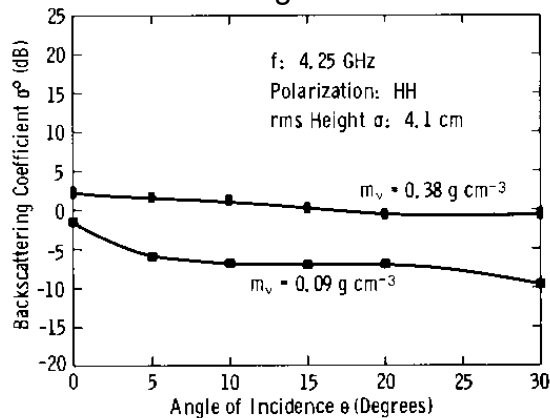
Smooth surface



Soil *roughness*: **angular** effect

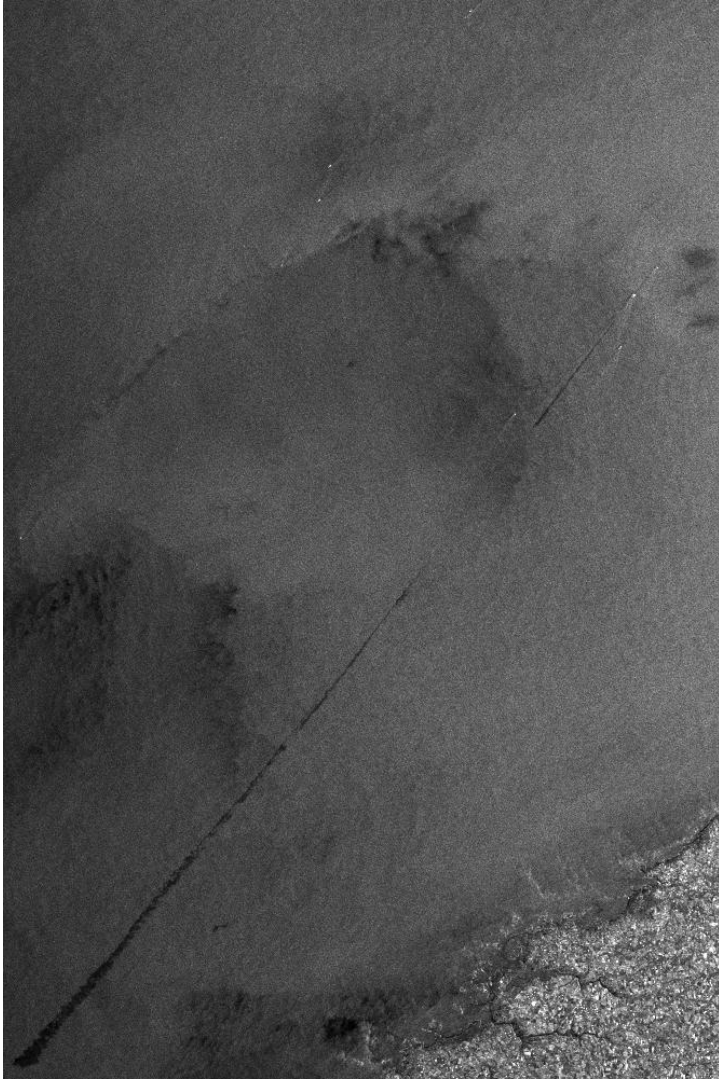
Soil *moisture*: **shift level** effect

Rough surface



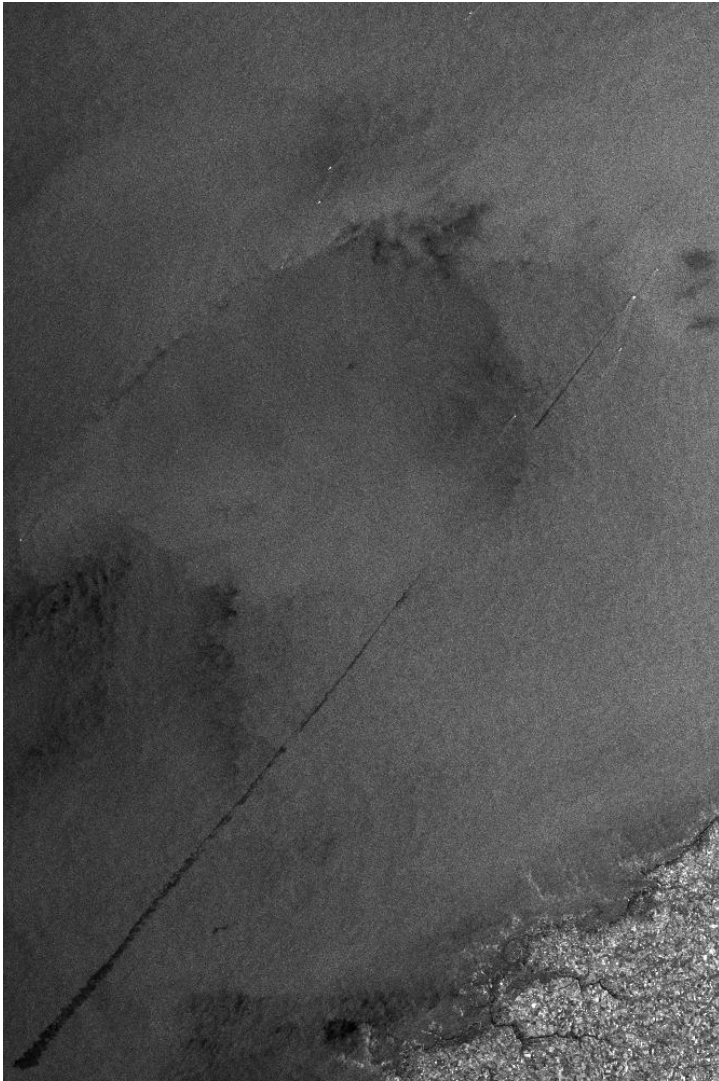
(b)

Radar response sensitivity



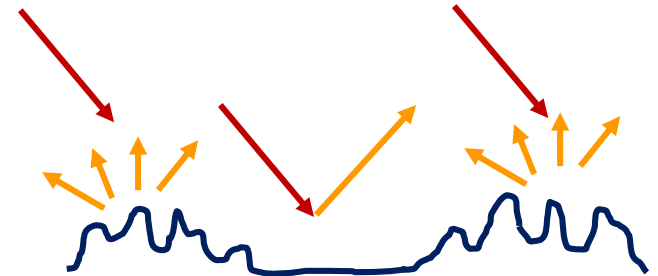
ERS (bande C, 23°, VV): 9 mars 1999

Radar response sensitivity



ERS (bande C, 23°, VV): 9 mars 1999

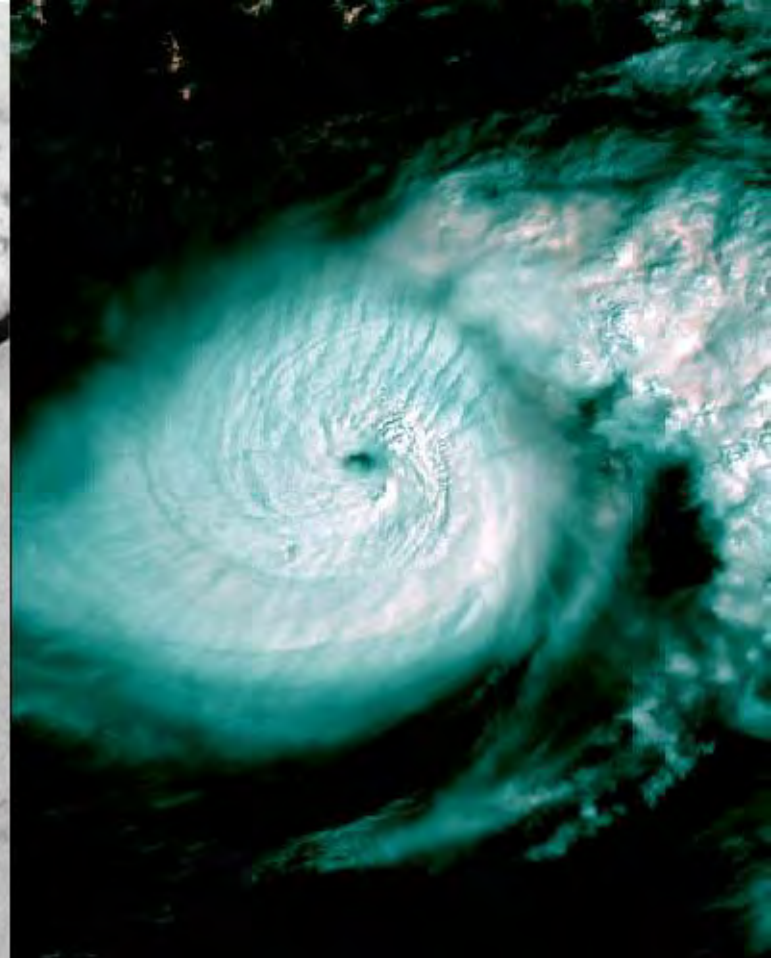
Over surface water:
surface roughness too



Typhon Isidore
Mexico - 21.09.2002



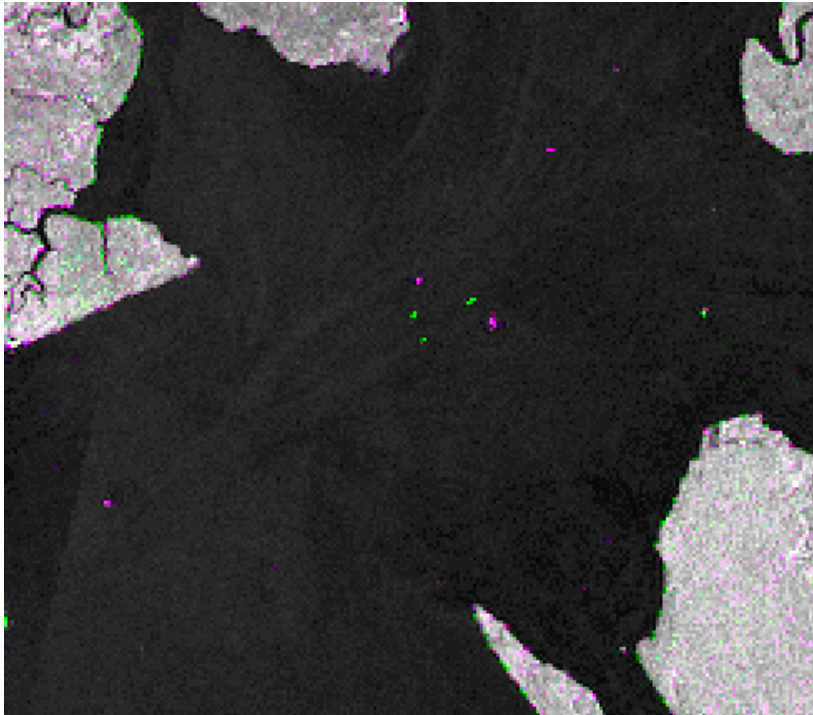
ASAR



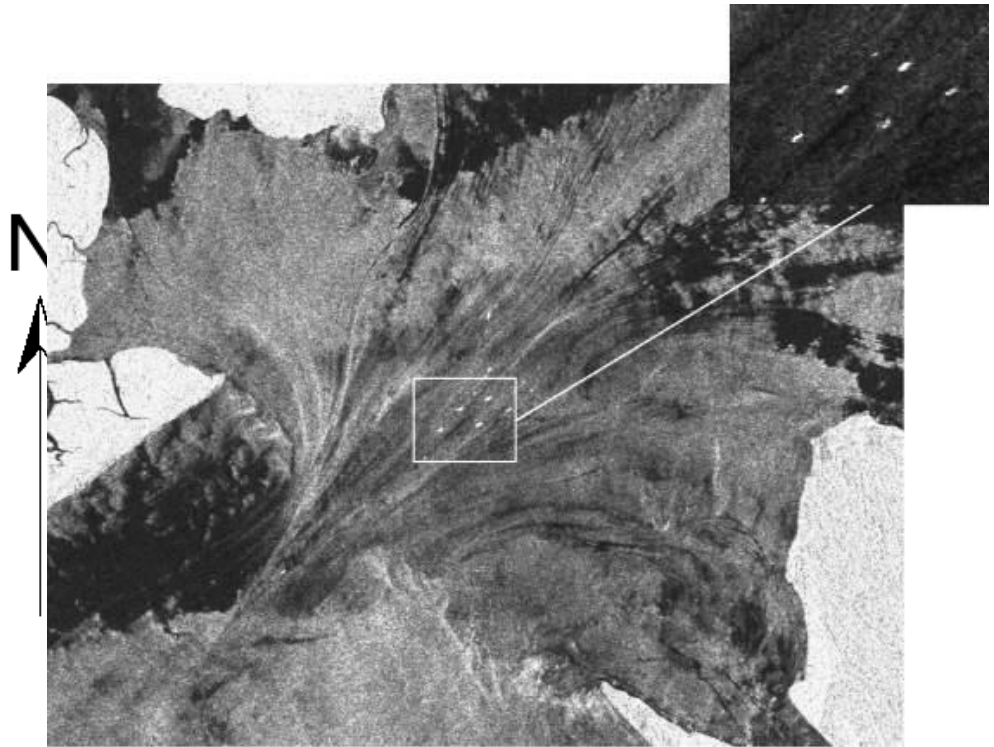
MERIS (600 m)

Frequency - wavelength

Exercise: why is it required to know the wavelength λ ?



JERS sensor
(Bande L, $\lambda = 25$ cm)



ERS sensor
(Bande C, $\lambda = 6$ cm)

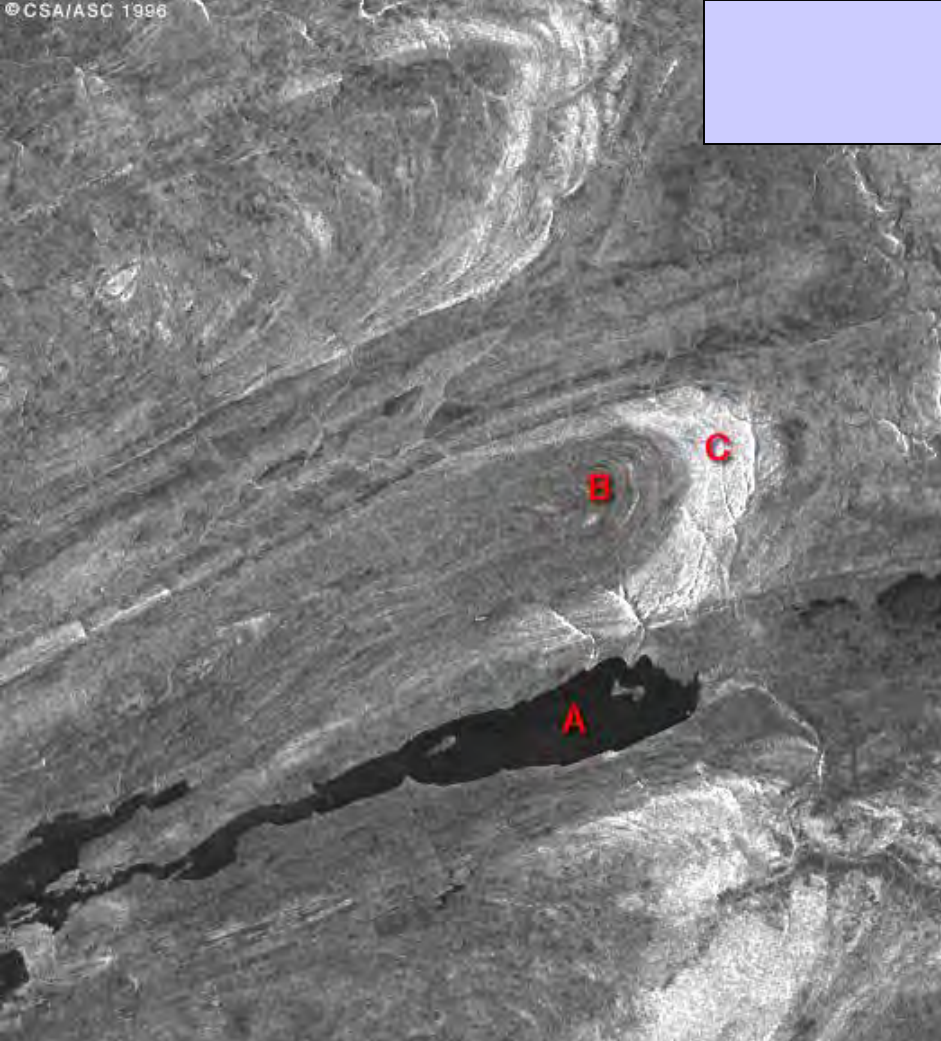
ERS radar image in Sahel



Over bare soil: depends on
Roughness
Soil moisture



Canada

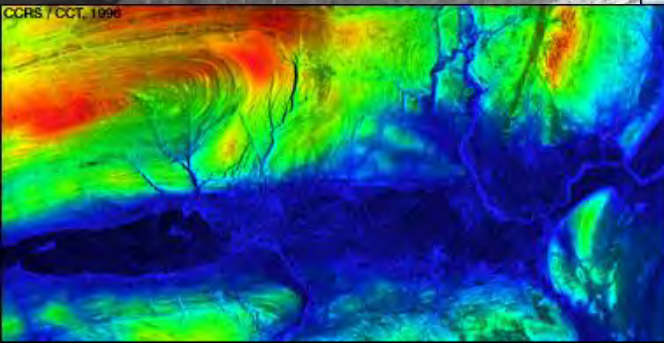


Siltstone 1.5 cm

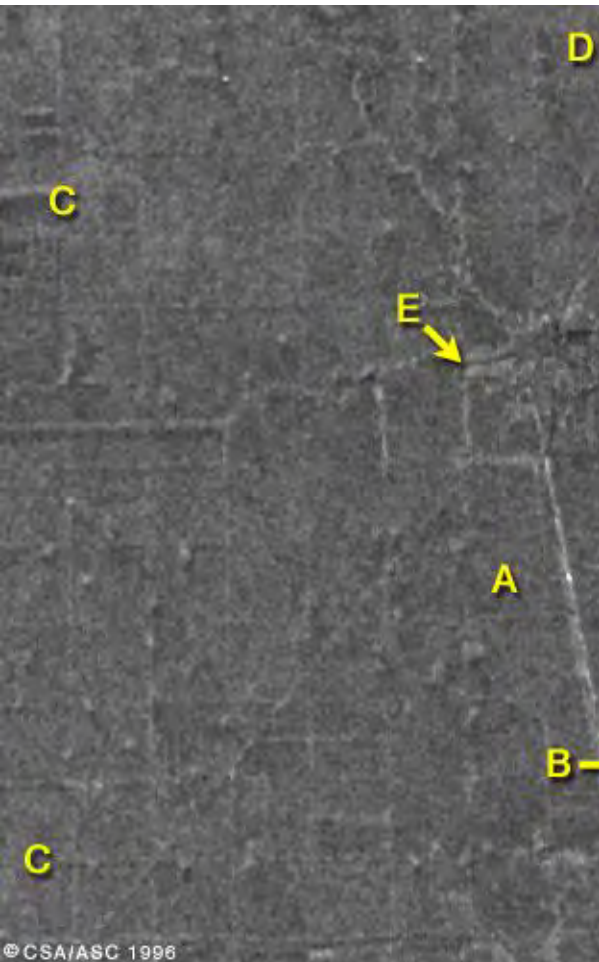
limestone 4.5cm



contact



Flooded areas monitoring



March 23 1996

The Red River, China



April 25 1996

Penetration effect

Radar ERS

optical



"Tin Etki"

Ain Cheik

Oued Temenasset

Desert Algeria

Effect of
penetration

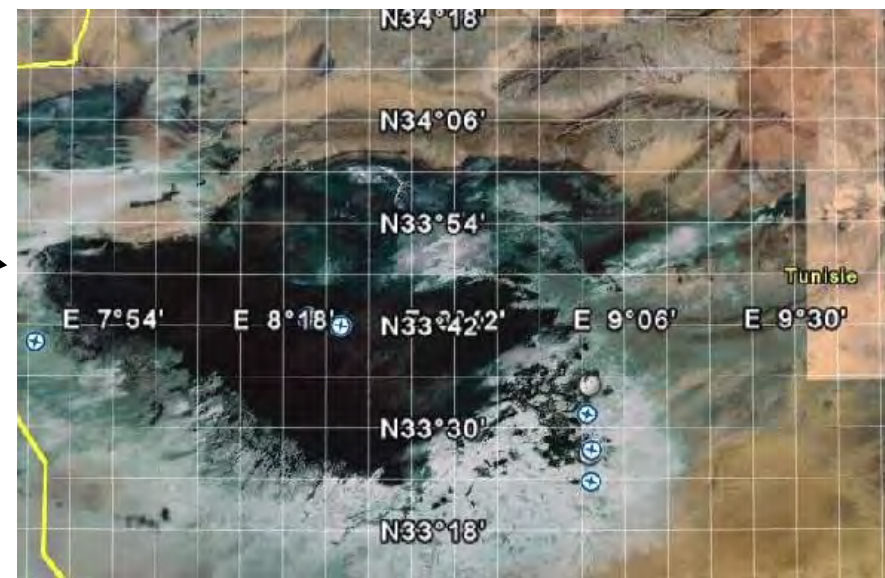
SIR A
band L



The Chott El Jerid, Tunisia



A vast evaporitic (80 x 120 km) area



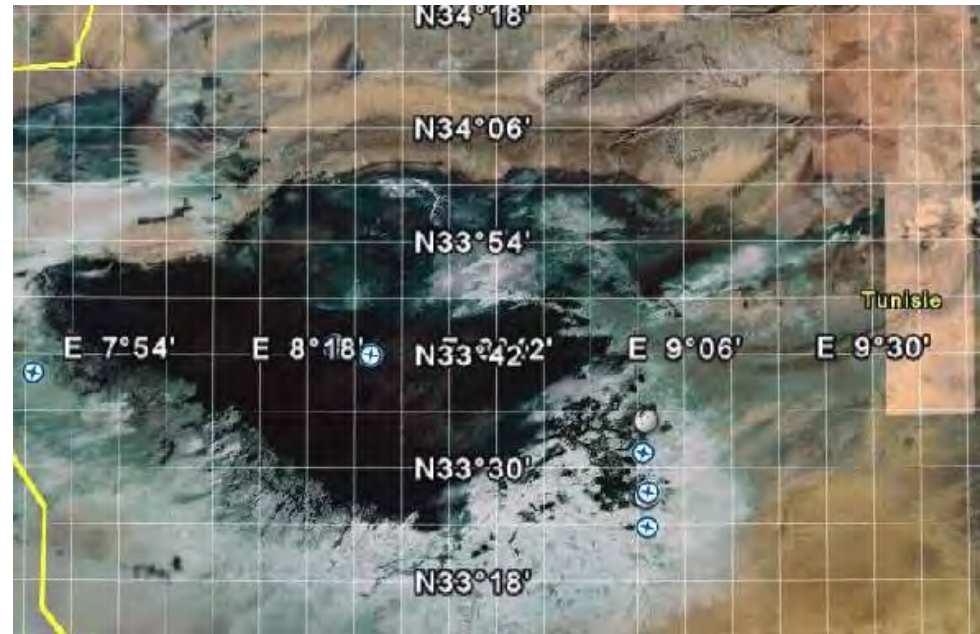
60 km

Discharge playa from a major aquifere
(upward percolation)

+
occasional runoff from neighbouring
playa (Fedjadj).

➔ *Temporary flooding*

Playas: Evaporites (saline deposits)



Flooded / dry surface

Wettest months

sudden smoothing due to dissolution of saline crust
+ dramatic change of diel. const. (saline solution)

Summer months:

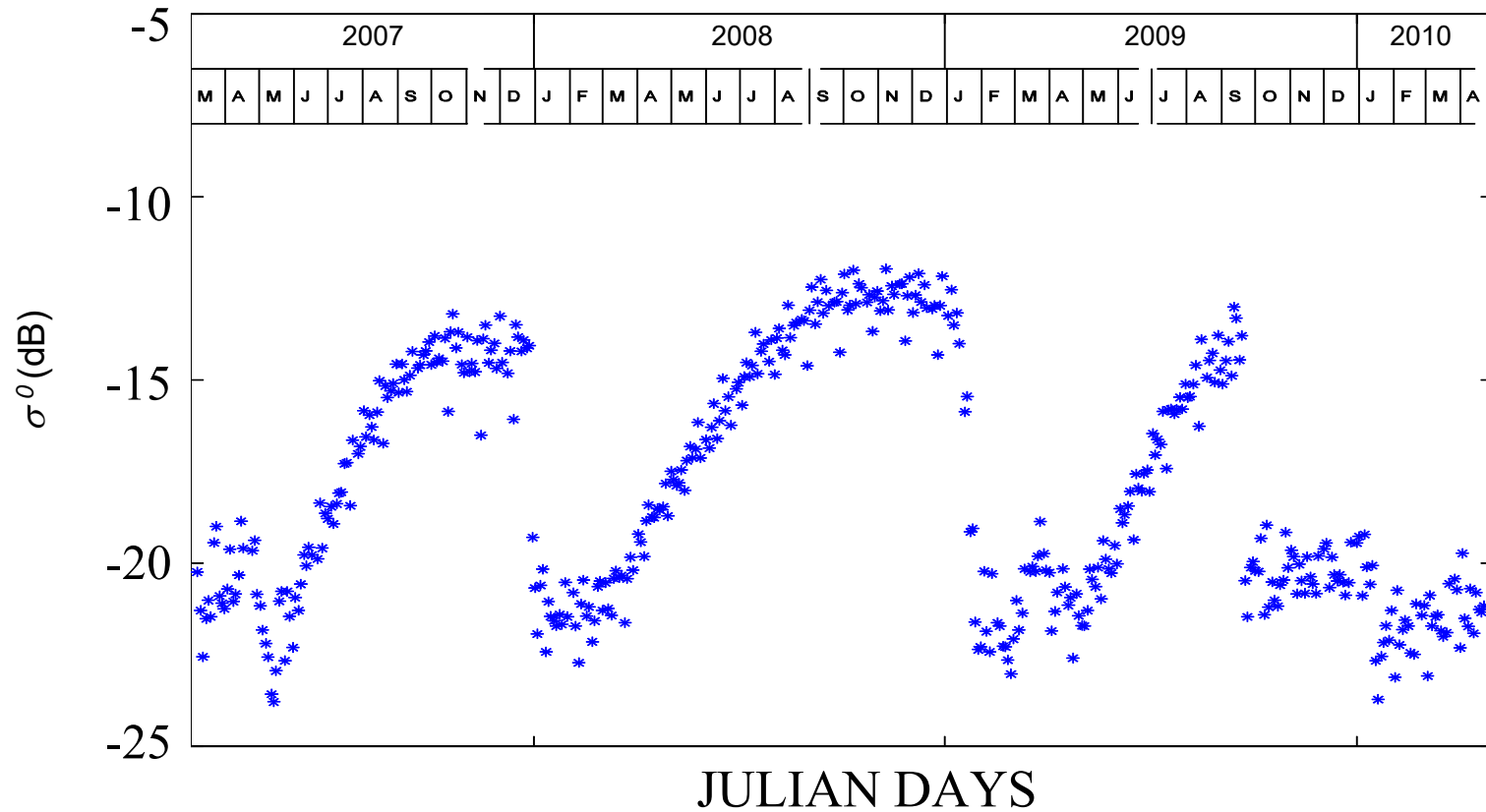
evaporation → halite crystal growth → increase of roughness

Lab and ground measurements, Death Valley
(roughness, dielectric constant)



ASCAT temporal signature over the Chott el Jerid

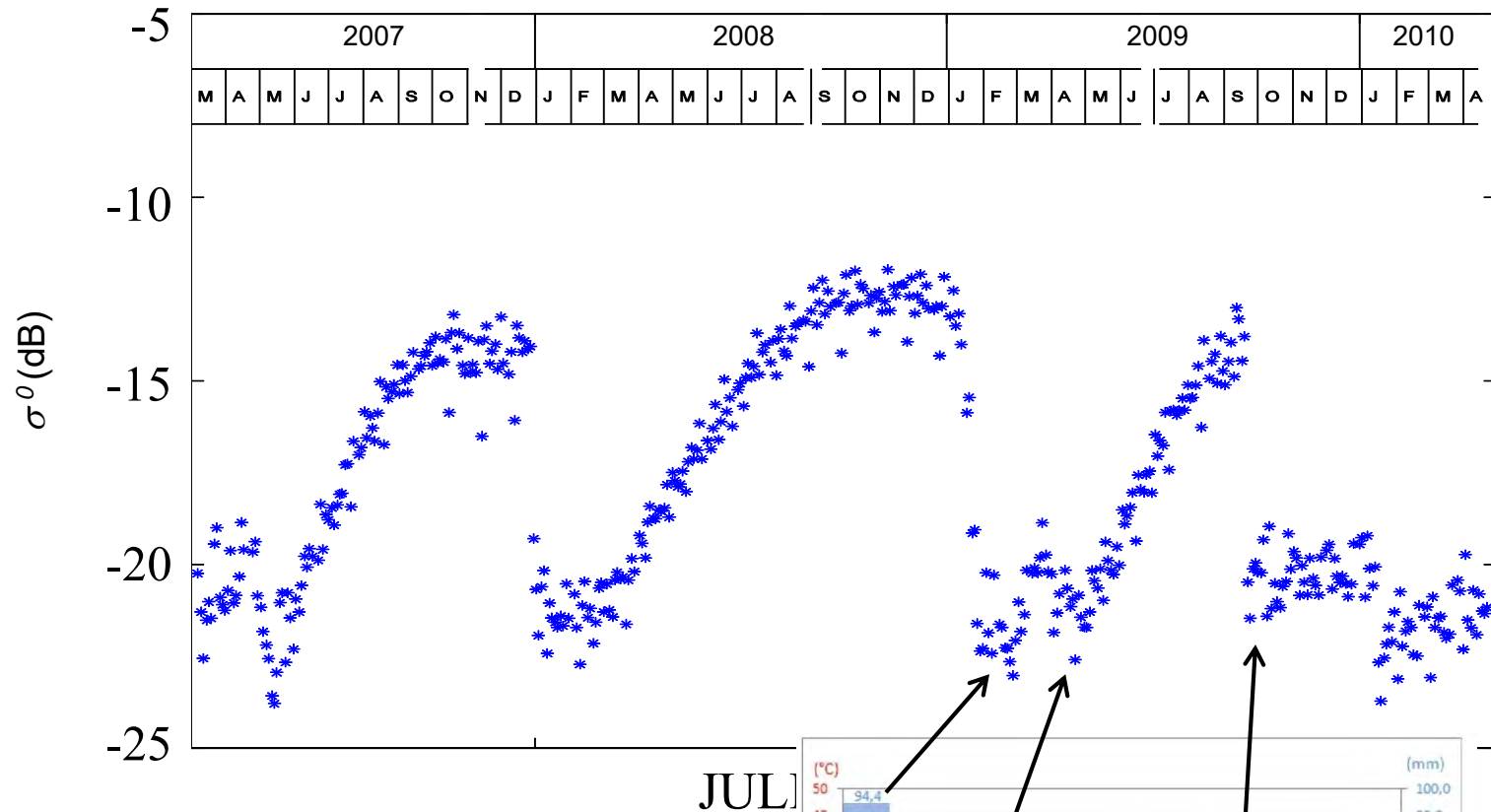
Incidence angle: 40°



High temporal dynamic (> 10 dB)
Linked to environment seasonal variations

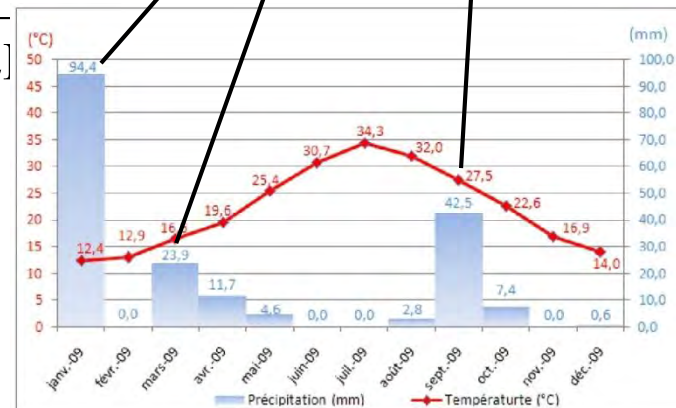
ASCAT temporal signature over the Chott el Jerid

Incidence angle: 40°



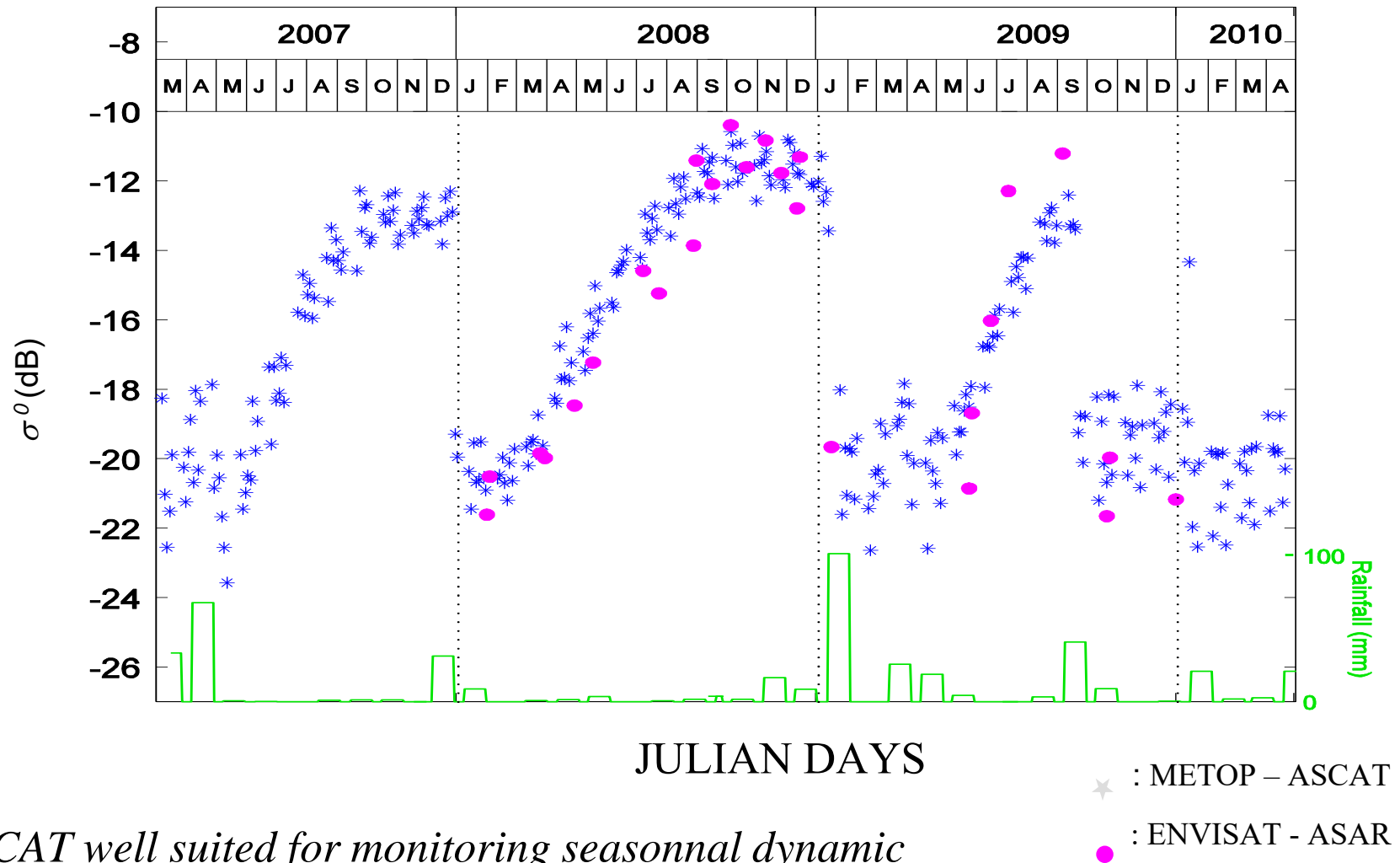
JUL

Precipitation, Tozeur, 2009

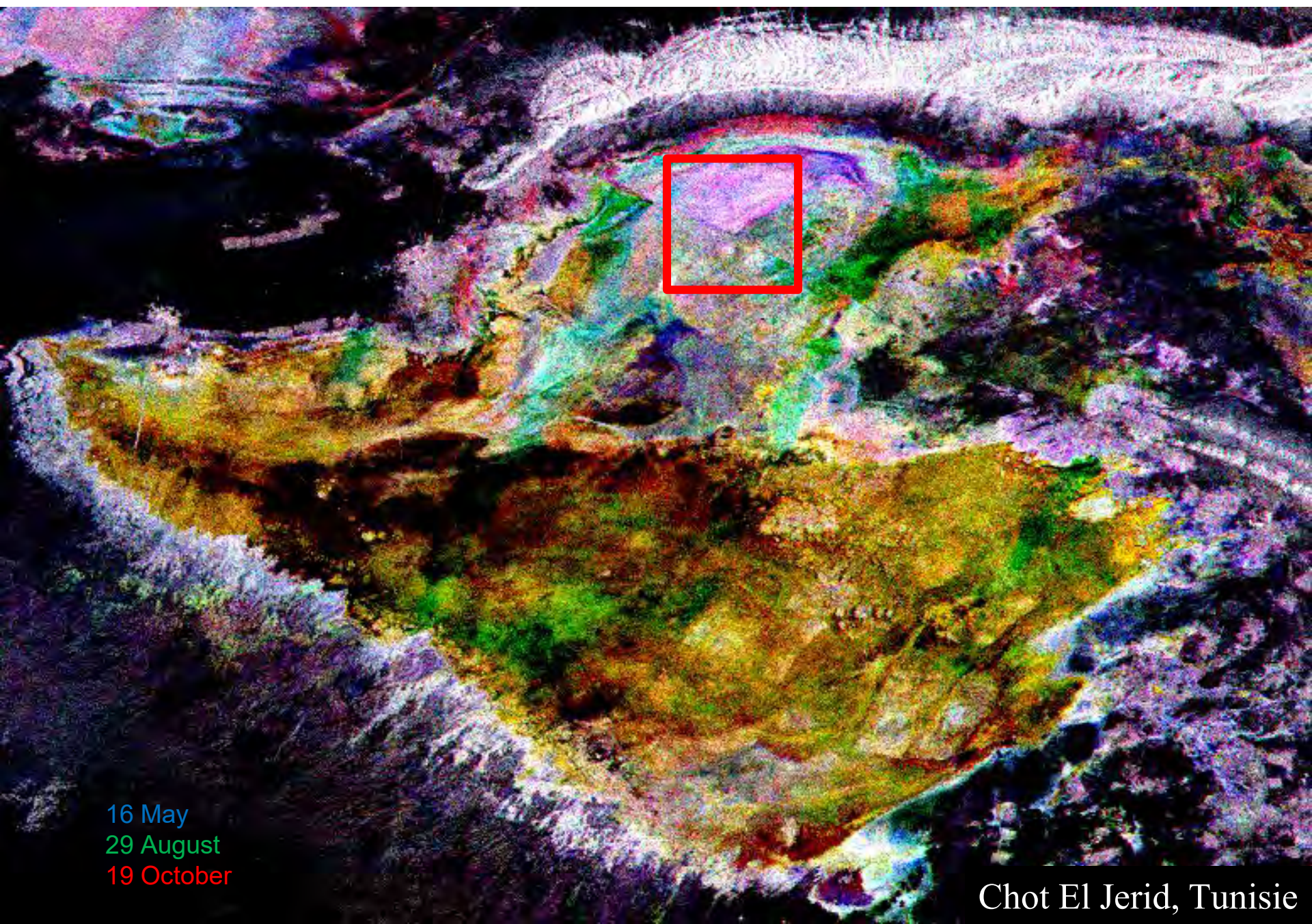


ASCAT/ASAR temporal signature over the Chott el Jerid

Incidence angle: 40°



ASCAT well suited for monitoring seasonal dynamic

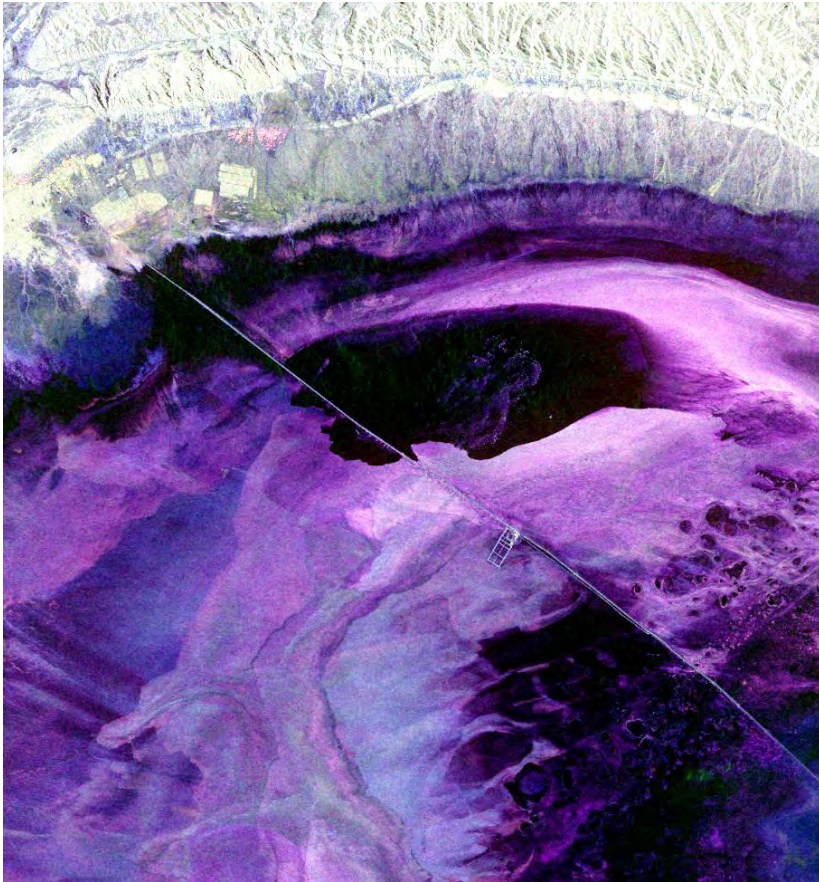


16 May
29 August
19 October

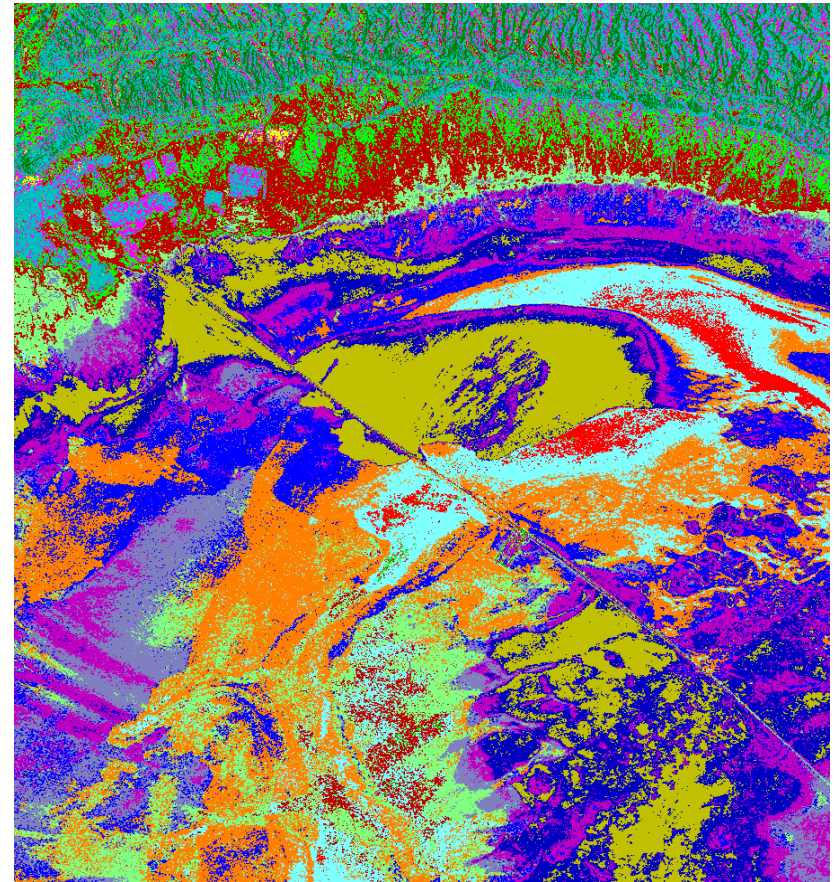
Chot El Jerid, Tunisie

Polarimetric data classification

Chott El Djerid



Decomposition de Pauli



Classification H/A/alpha

Radarsat-2 - 17 avril 2009

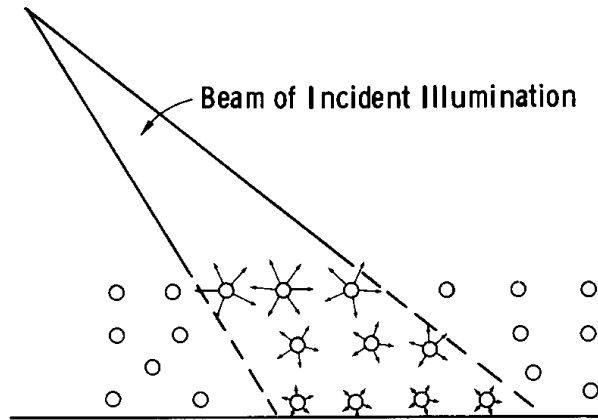
Radar response sensitivity

Over vegetation

Volume scattering

Radar images interpretation rules

Volume scattering



Inhomogeneous medium (vegetation cover)

each inhomogeneity (leaves, branches....)
scatters incident wave in all direction

Multiple scattering
+
Absorption } ==> wave attenuation within the layer

Radar images interpretation rules

Volume scattering

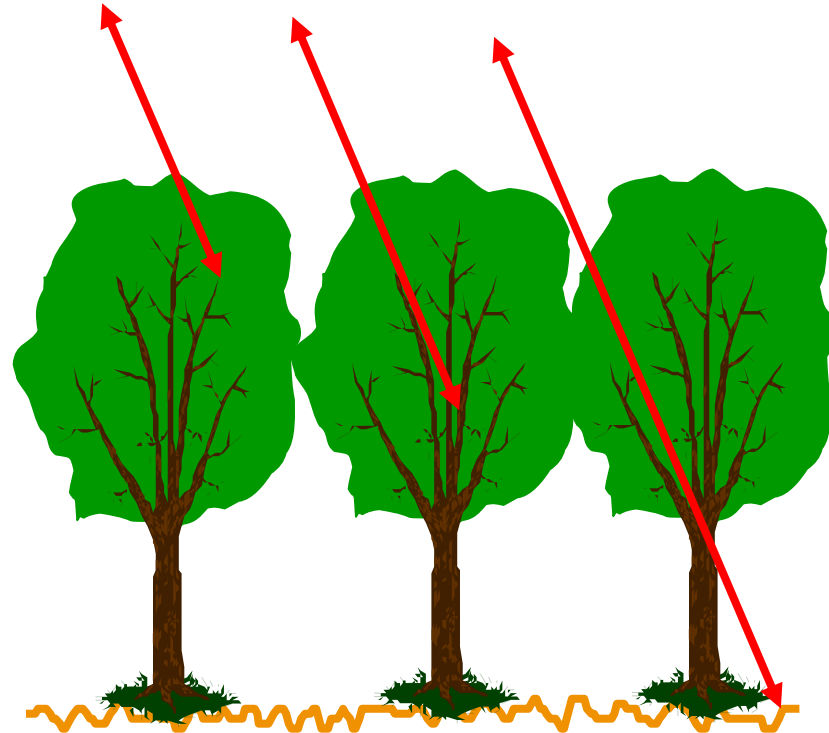
C band

L band

P-band

Penetration Depth:

$$\delta = \frac{\lambda}{4 \pi \operatorname{Im}(\sqrt{\varepsilon})}$$



Penetration \nearrow { Biomass \searrow
wavelength \nearrow

Bande C

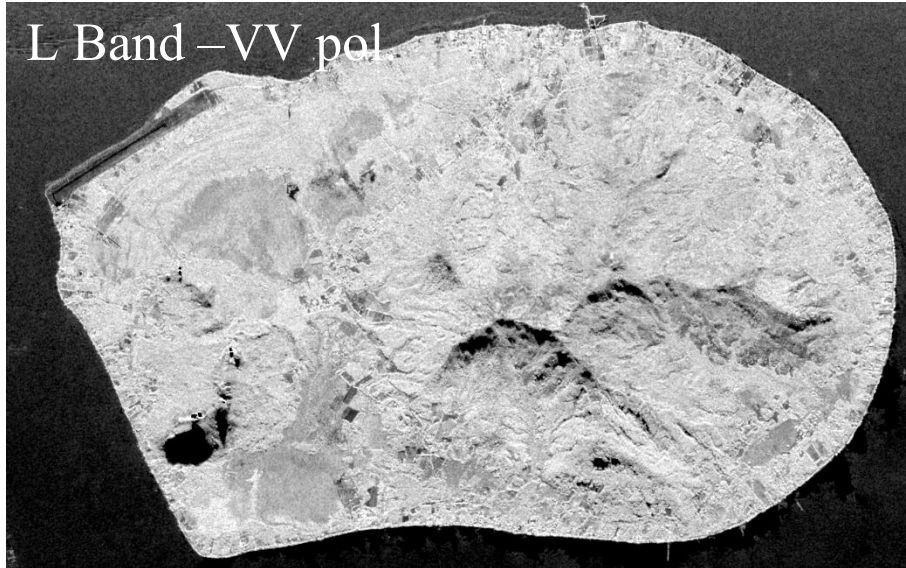


Radar response over French Guiana

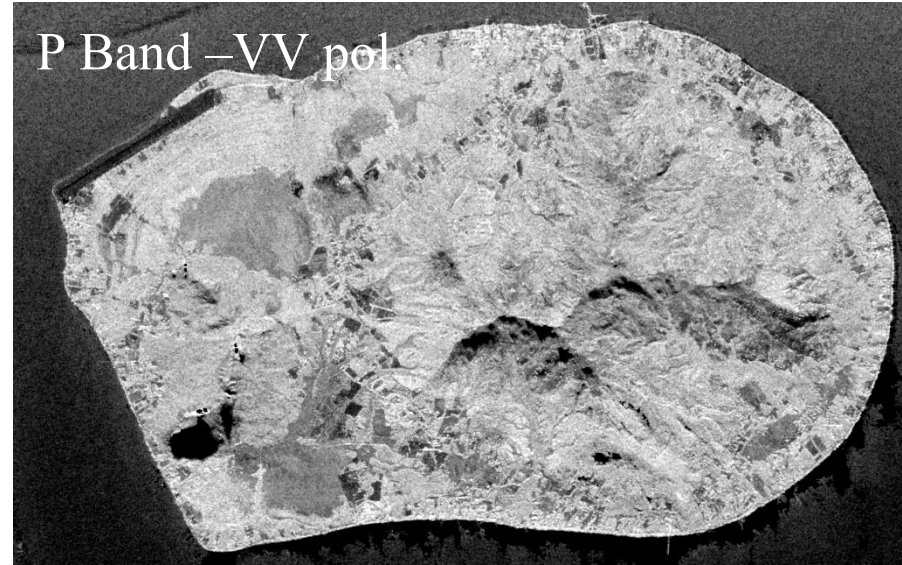
Frequency - wavelength

Tubuai Island, Vegetation discrimination

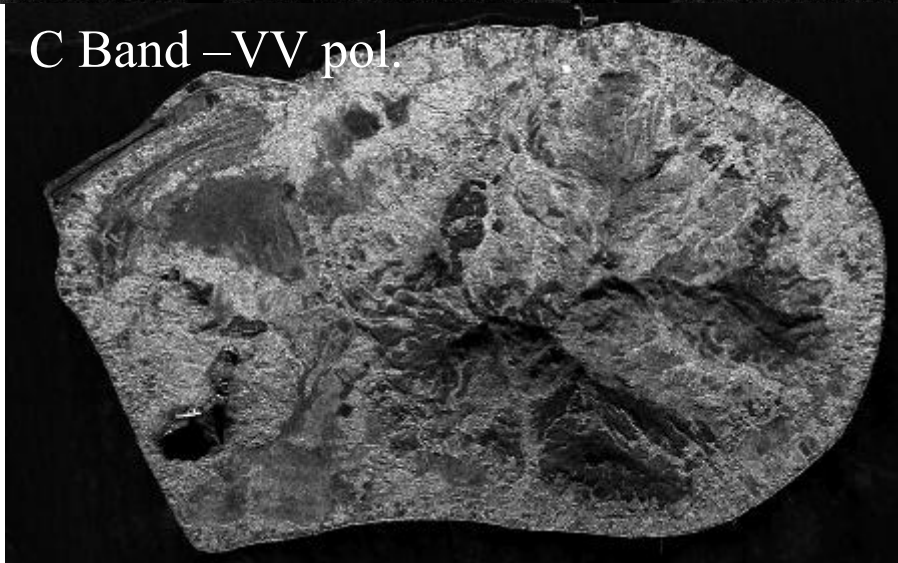
L Band –VV pol.



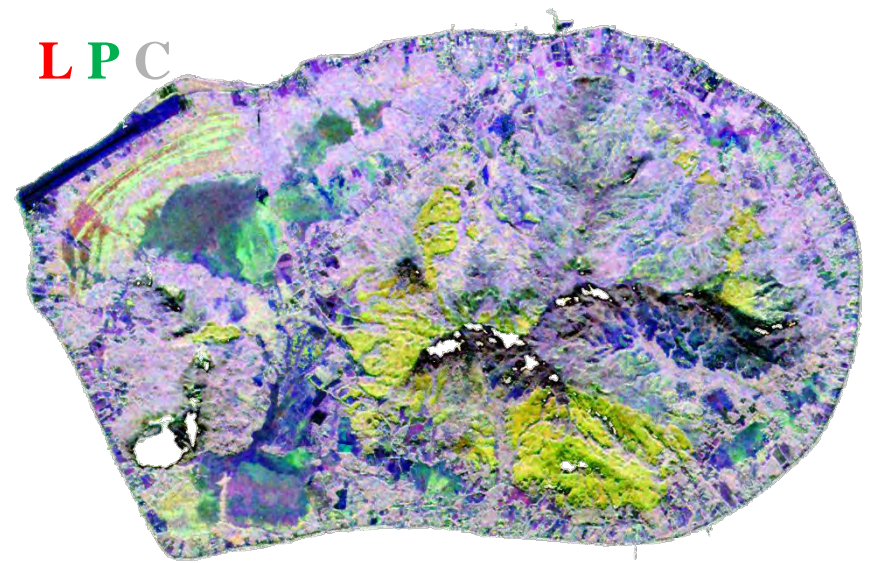
P Band –VV pol.



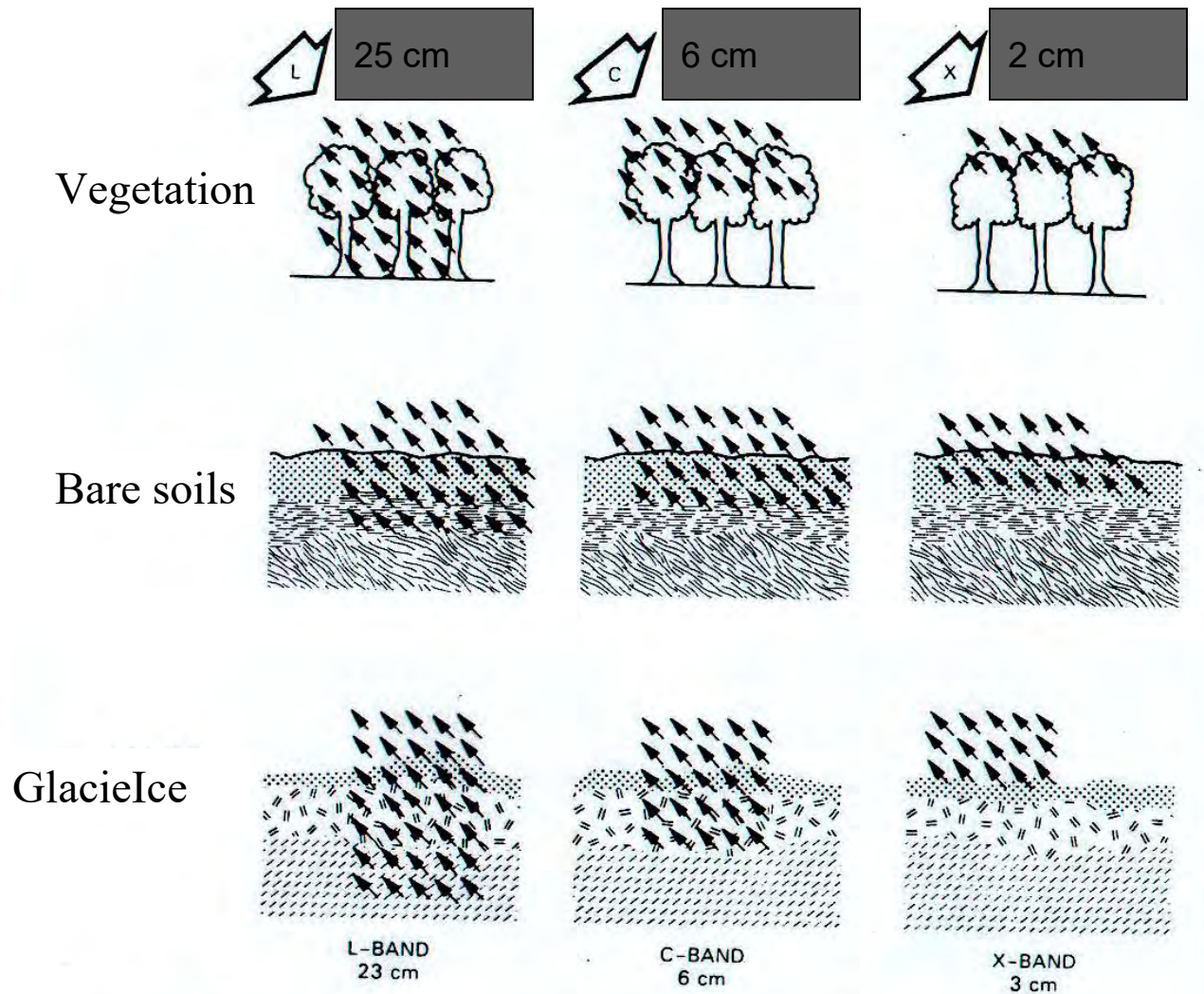
C Band –VV pol.



L P C

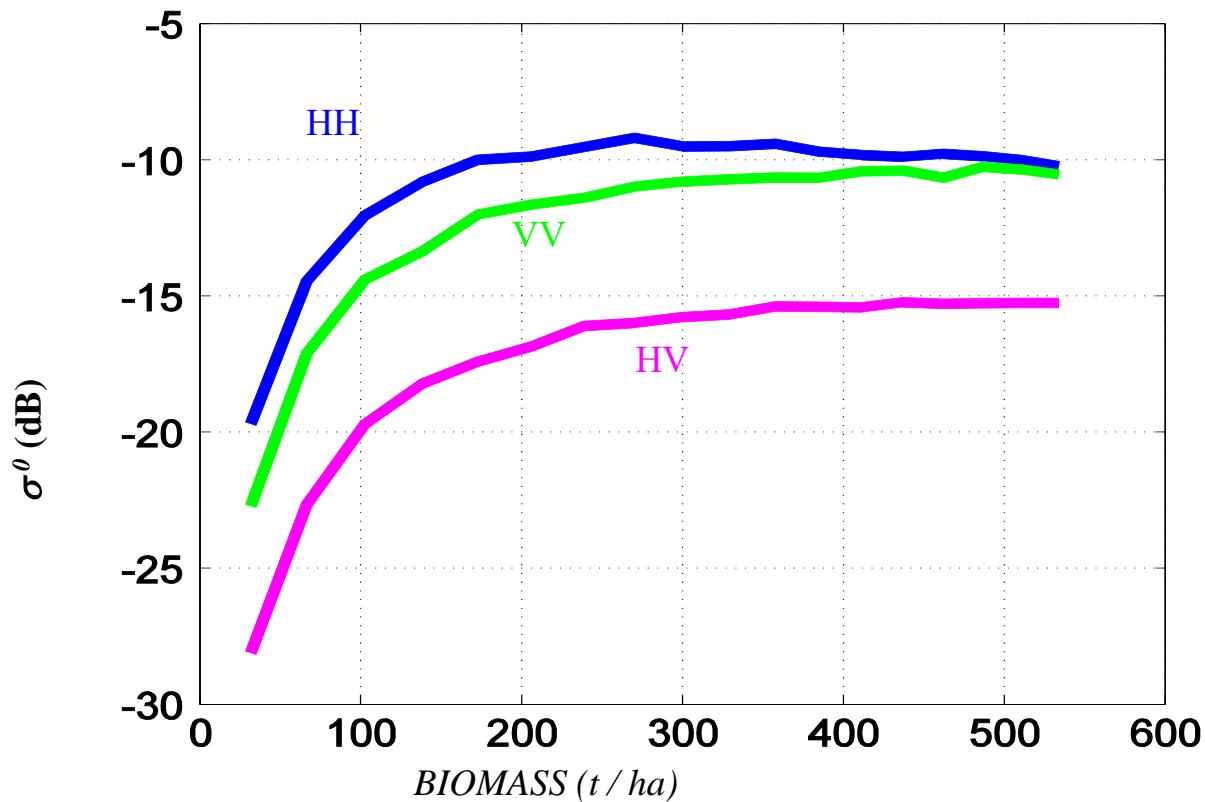


Radar response sensitivity



Radar images interpretation rules

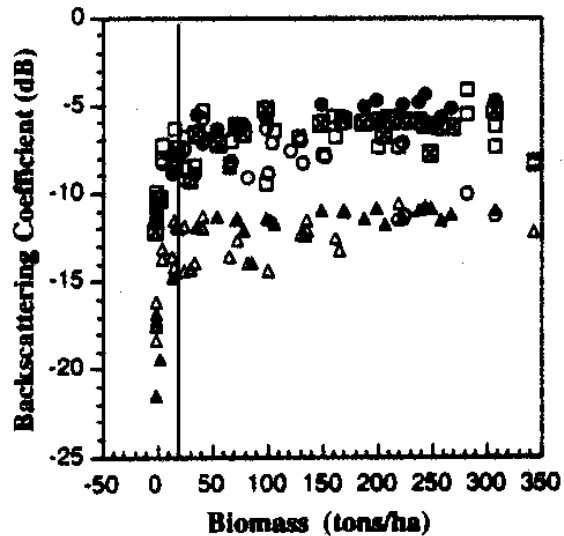
Radar response over forest



Volume Scattering

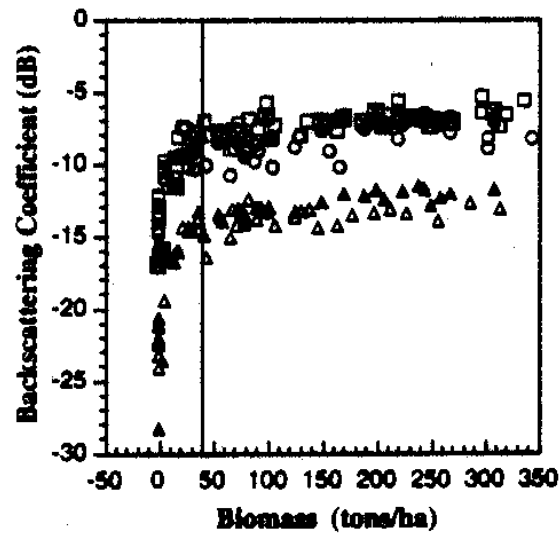
Radar saturation level with vegetation density

C band



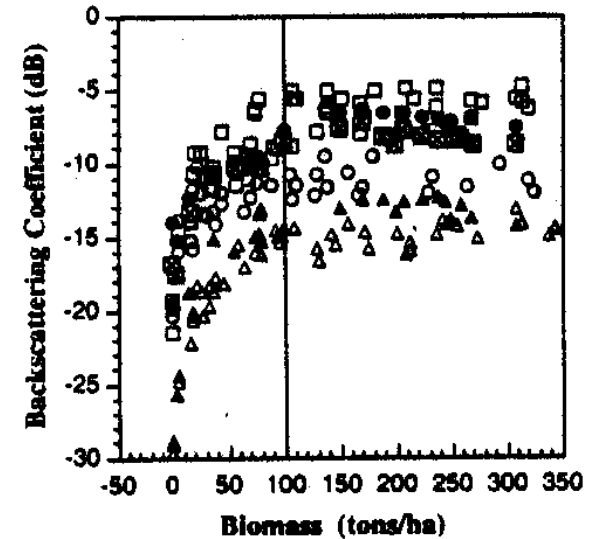
20 tons/ha

L band



40 tons/ha

P band

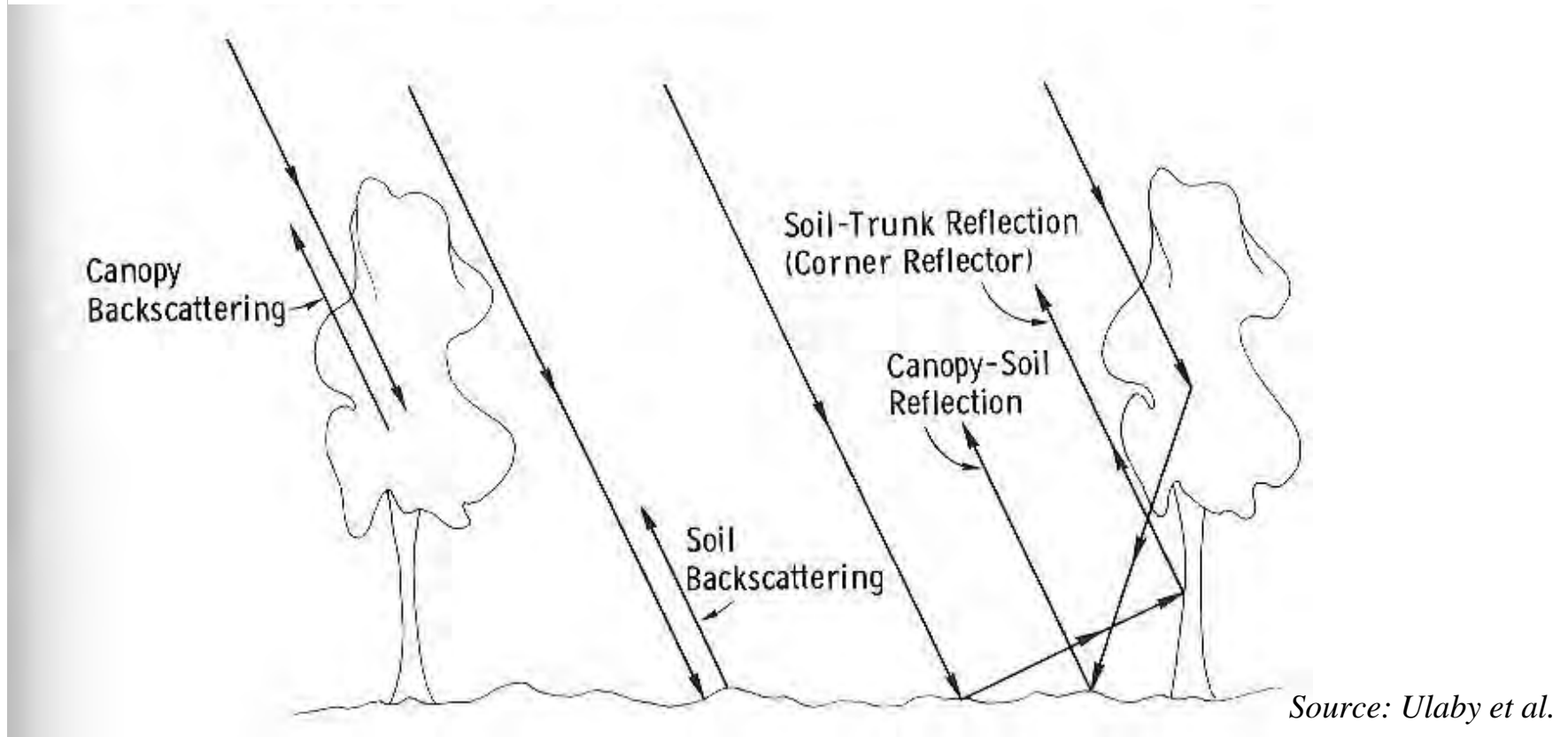


100 tons/ha

from Imhoff et al. 19?

Radar response sensitivity

Backscattering mechanism on vegetation

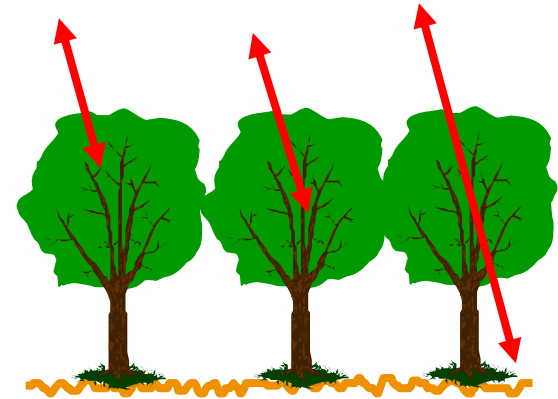


Land surfaces monitoring with radar data

Radar observations sensibility

- ☞ Biomass
- ☞ Structure and moisture of vegetation
- ☞ Roughness and moisture of soils

$\lambda = 6 \text{ cm}$ $\lambda = 25 \text{ cm}$ $\lambda = 70 \text{ cm}$



Access to key variables of ecosystem functioning

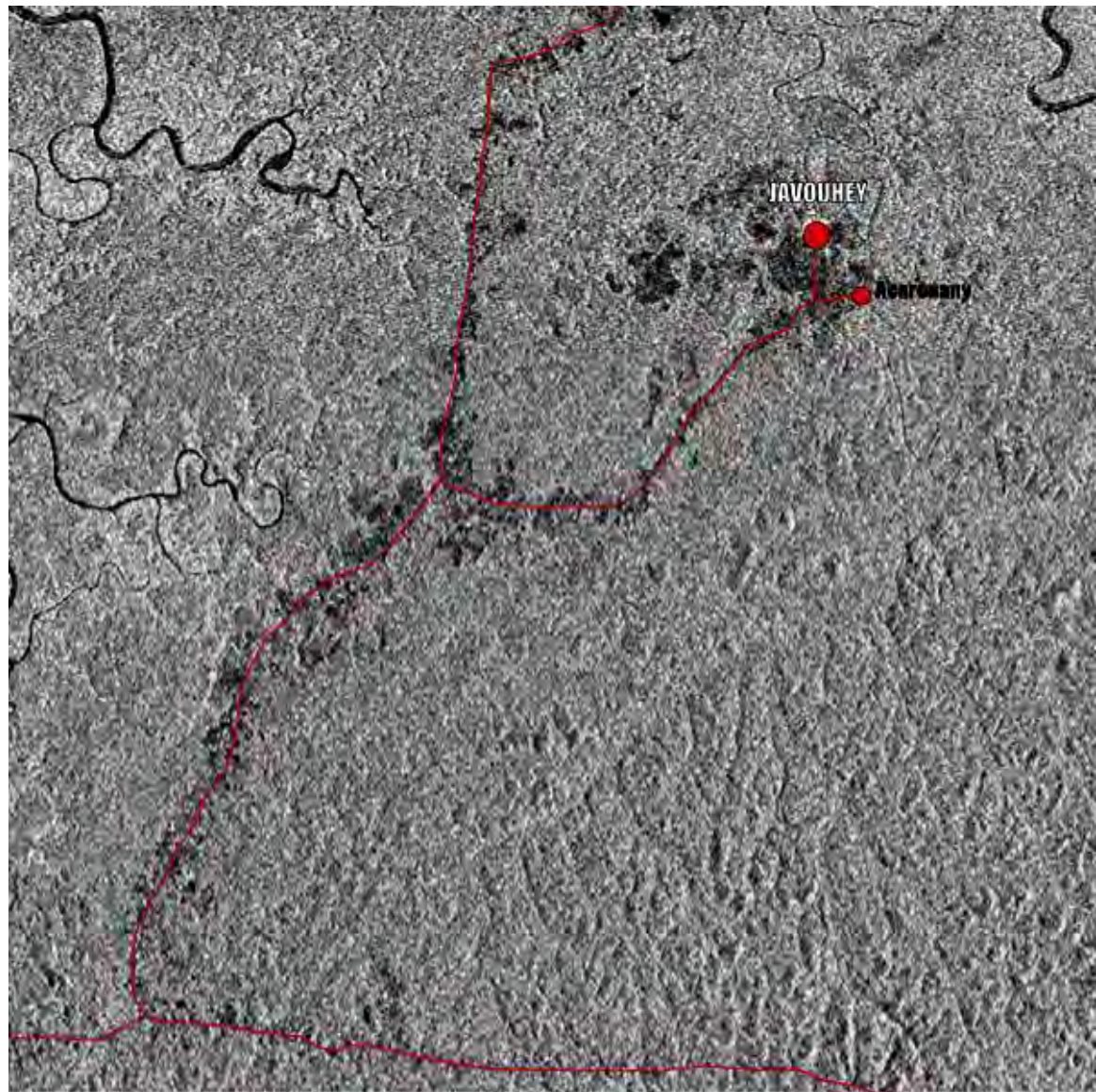
- ☞ Vegetation discrimination (type, espèces, état,...)
- ☞ Biomass (Net Primary Productivity)
- ☞ Vegetation phenology (periods of activity)
- ☞ Hydrological states of plant covers (stress,)
- ☞ Soil moisture

Radar response sensitivity

Local Agricultural Deforestation along road



Radar response sensitivity



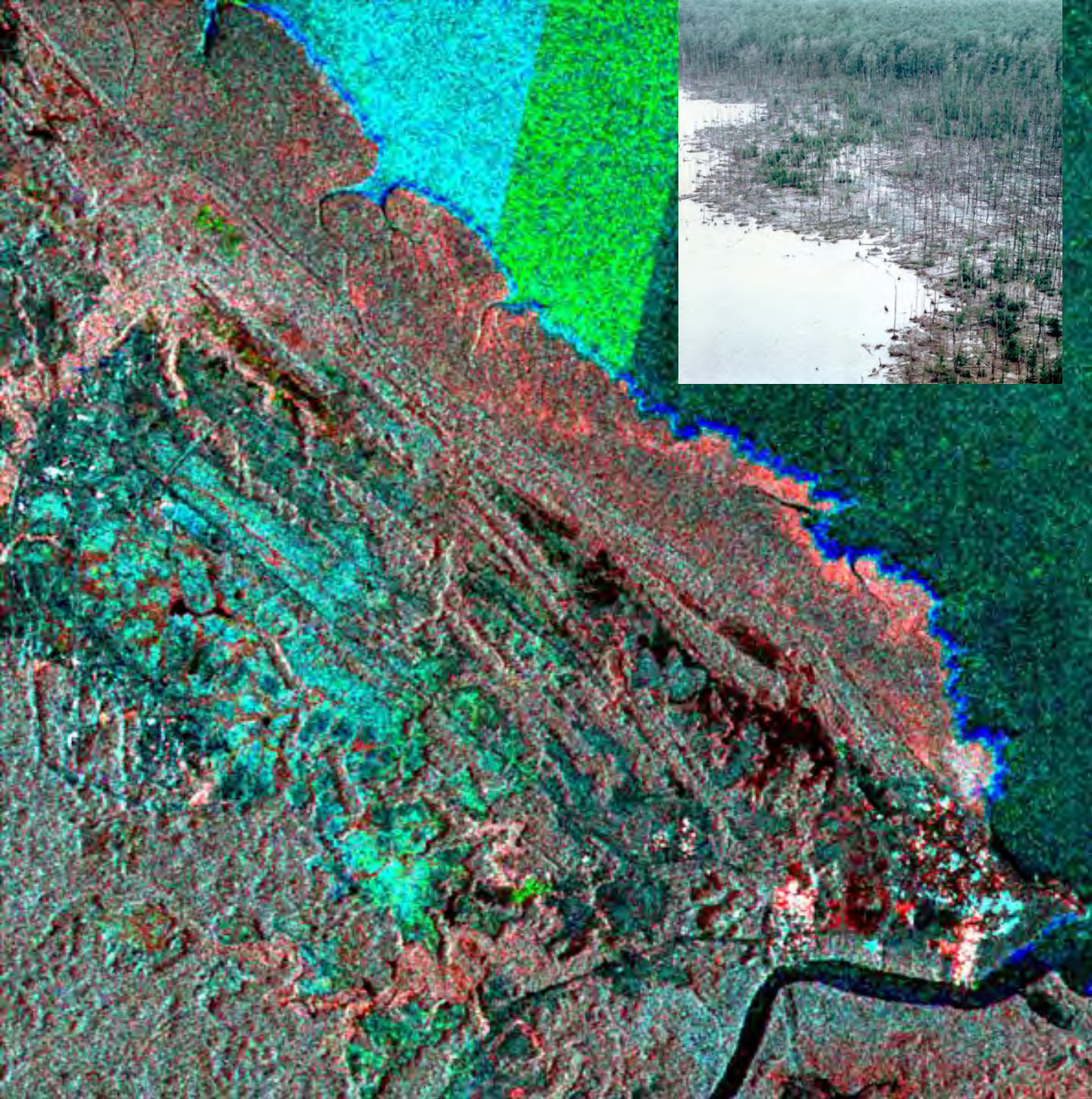
Radar response sensitivity

Cameroun (Ngaoundéré région : Cultural practice, burned area





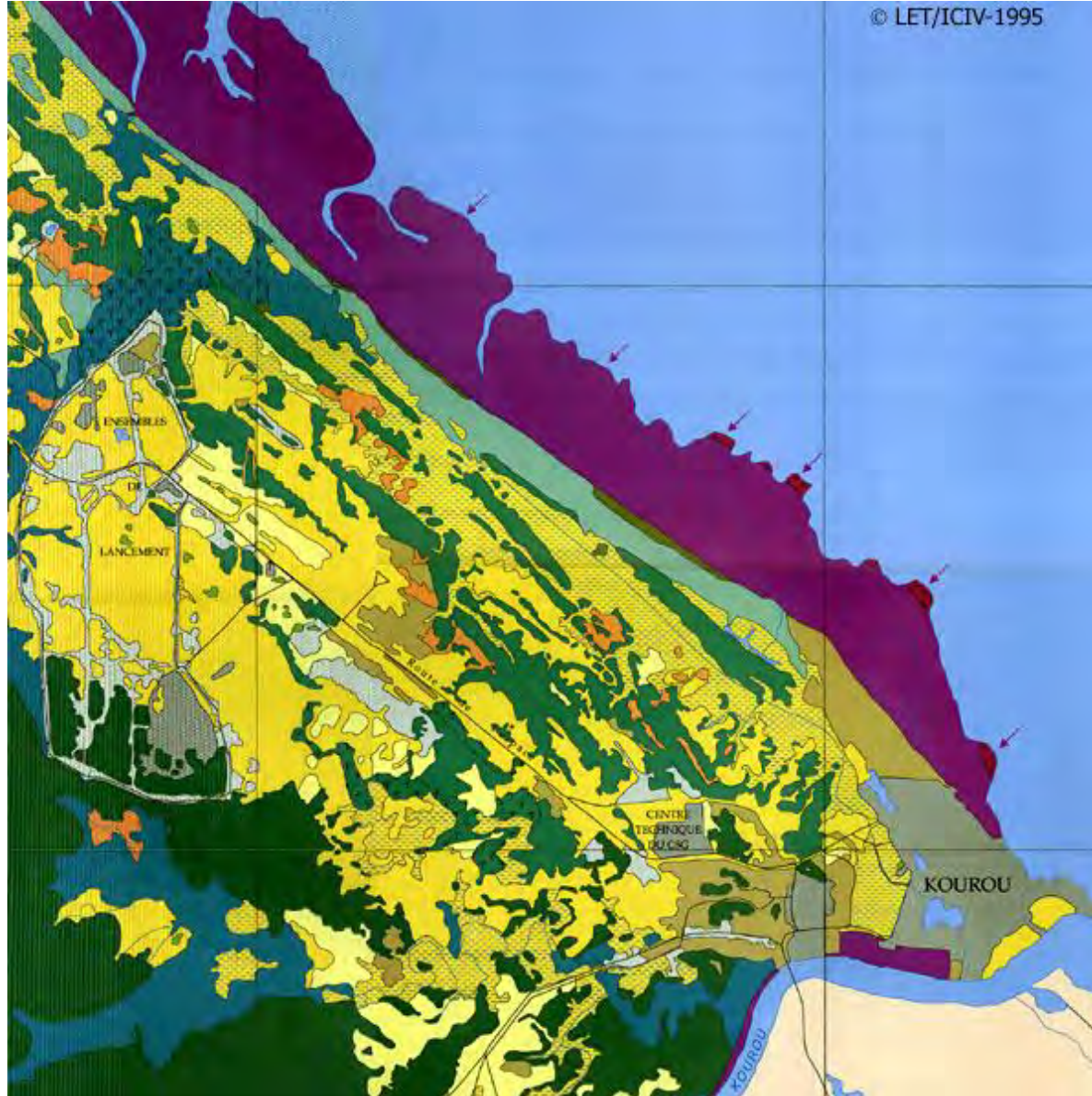
Dry season



Color Composite

ERS and **JERS**

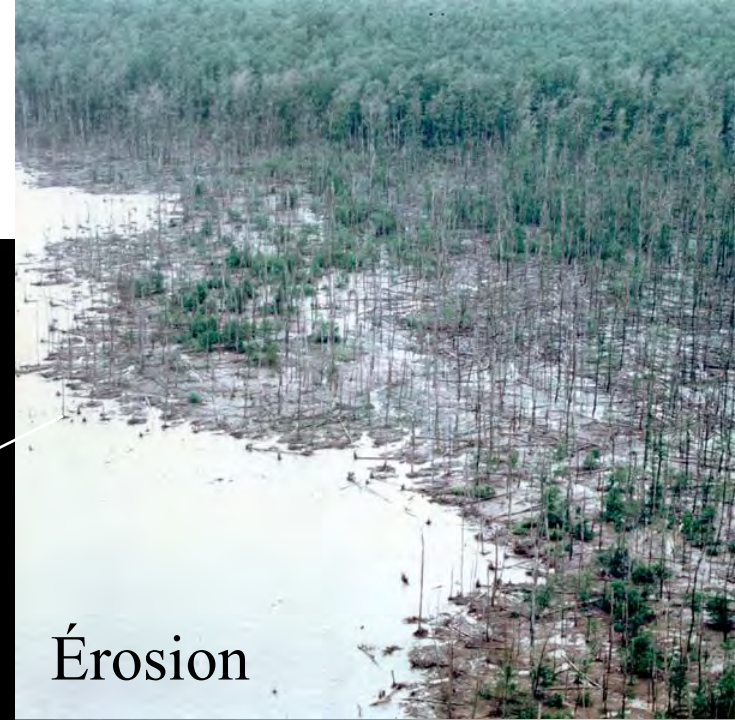
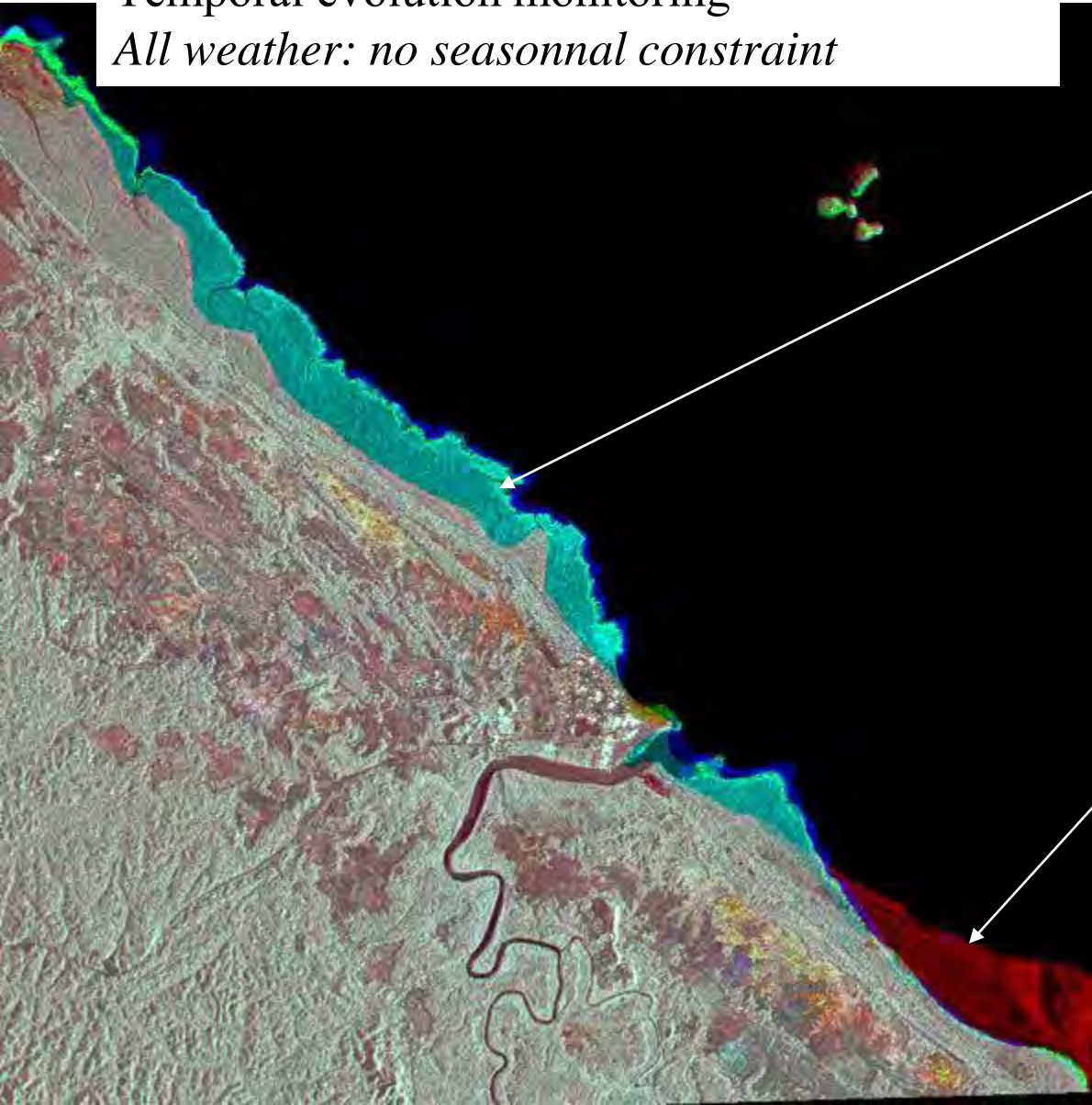
Radar response sensitivity



Radar response sensitivity

Temporal evolution monitoring

All weather: no seasonal constraint



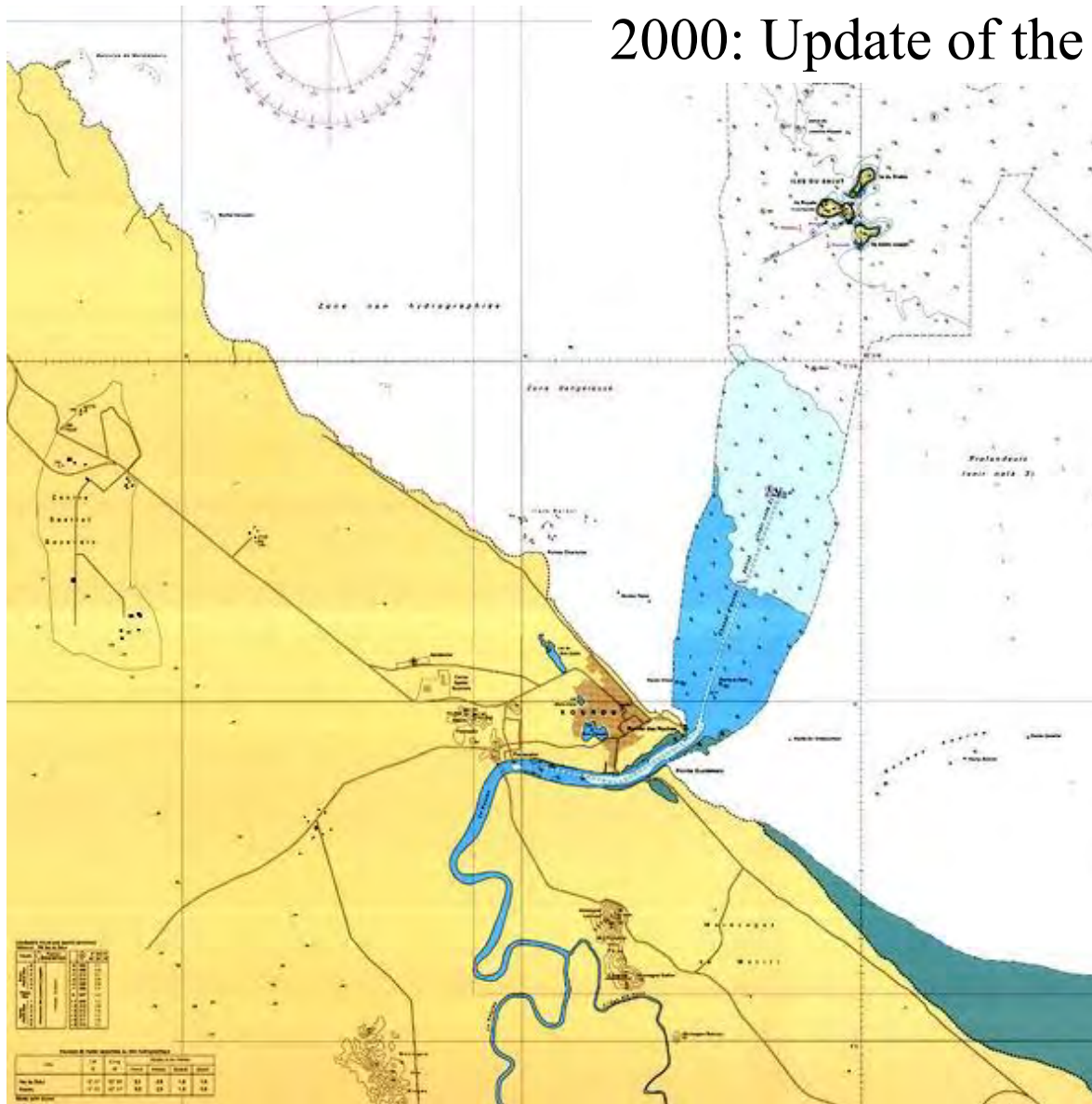
Érosion



Sédimentation

Radar response sensitivity

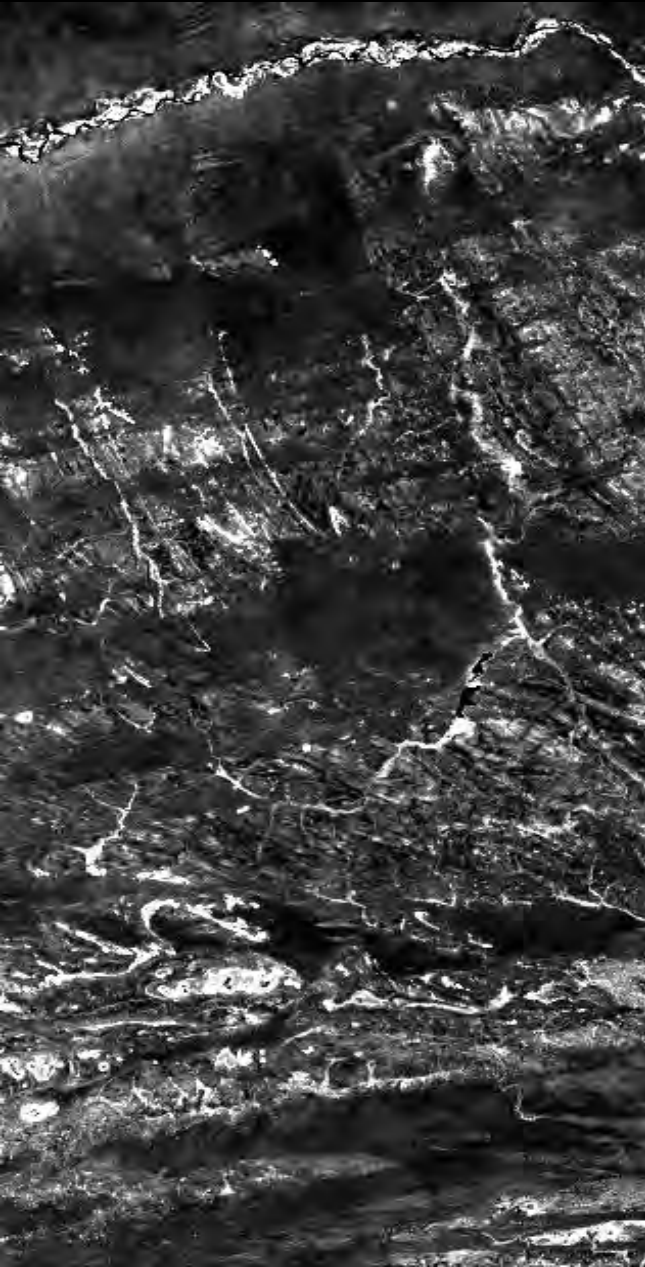
2000: Update of the marine map



Source: SHOM/ Univ-MLV

Seasonal variations monitoring (Sahel)

ASAR ($\lambda = 6$ cm)

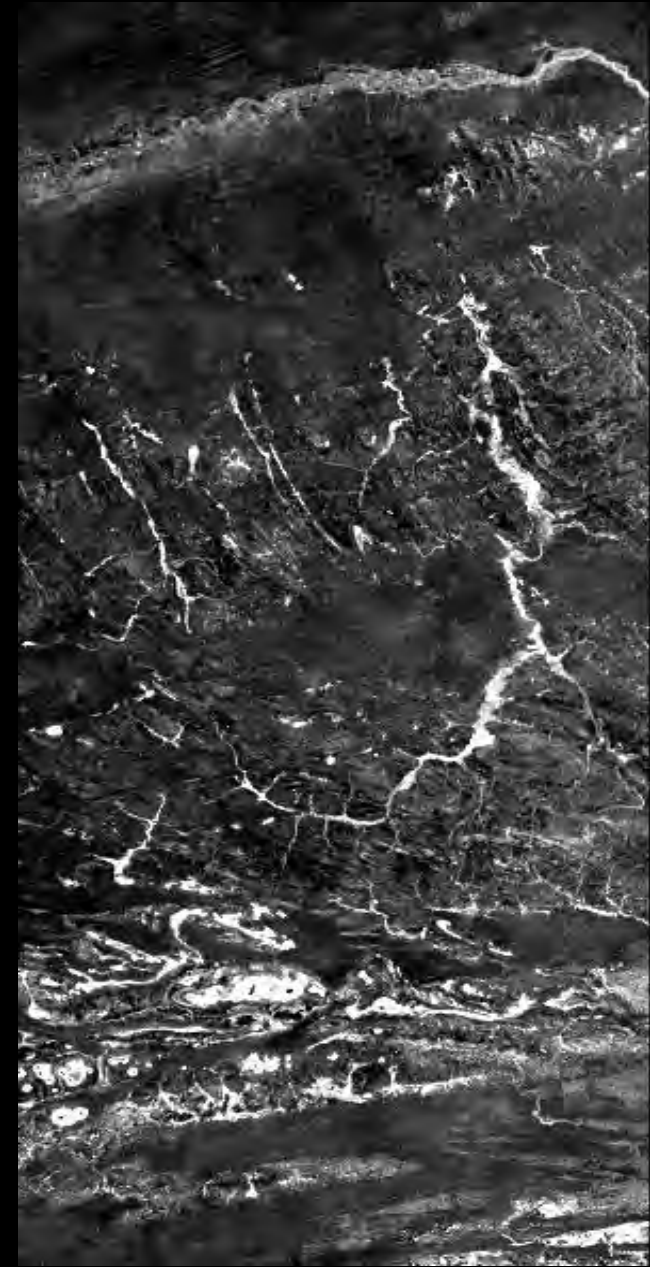


C Band (ASAR):
Sensitive to sandy and silty soils

Bande L (PALSAR):
*Better discrimination
of geological structures*

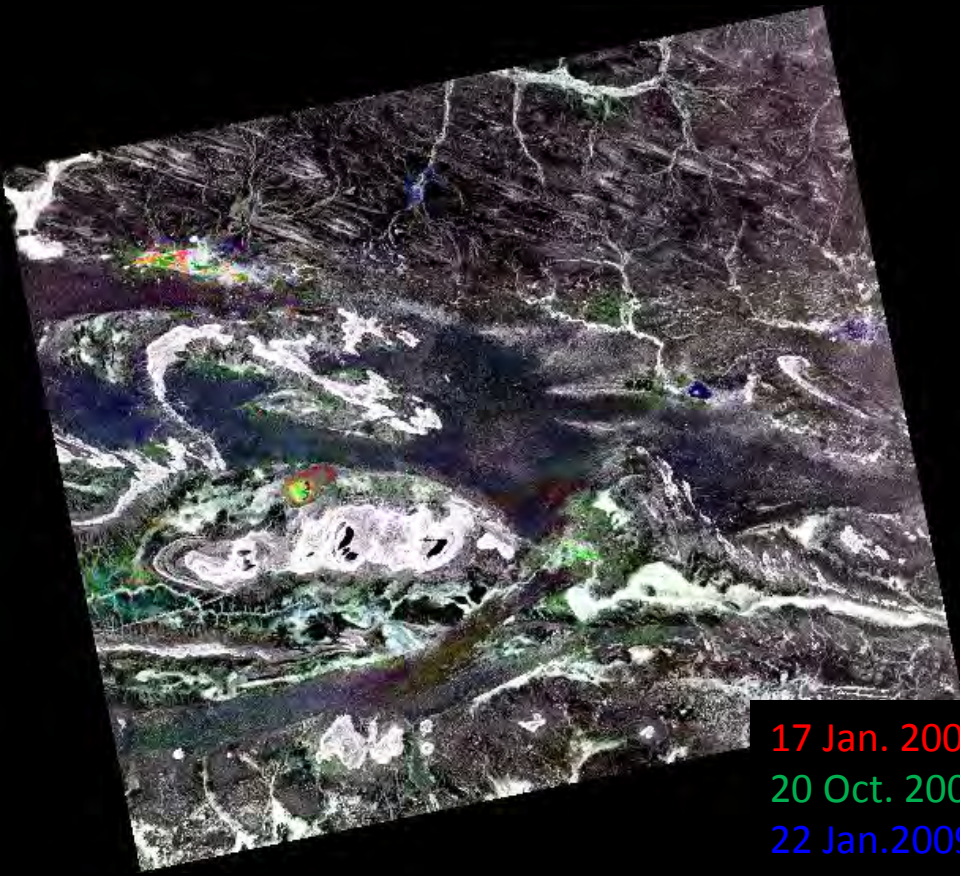
*Remnant of alluvial system
and lacustrine depressions*

PALSAR ($\lambda = 24$ cm)



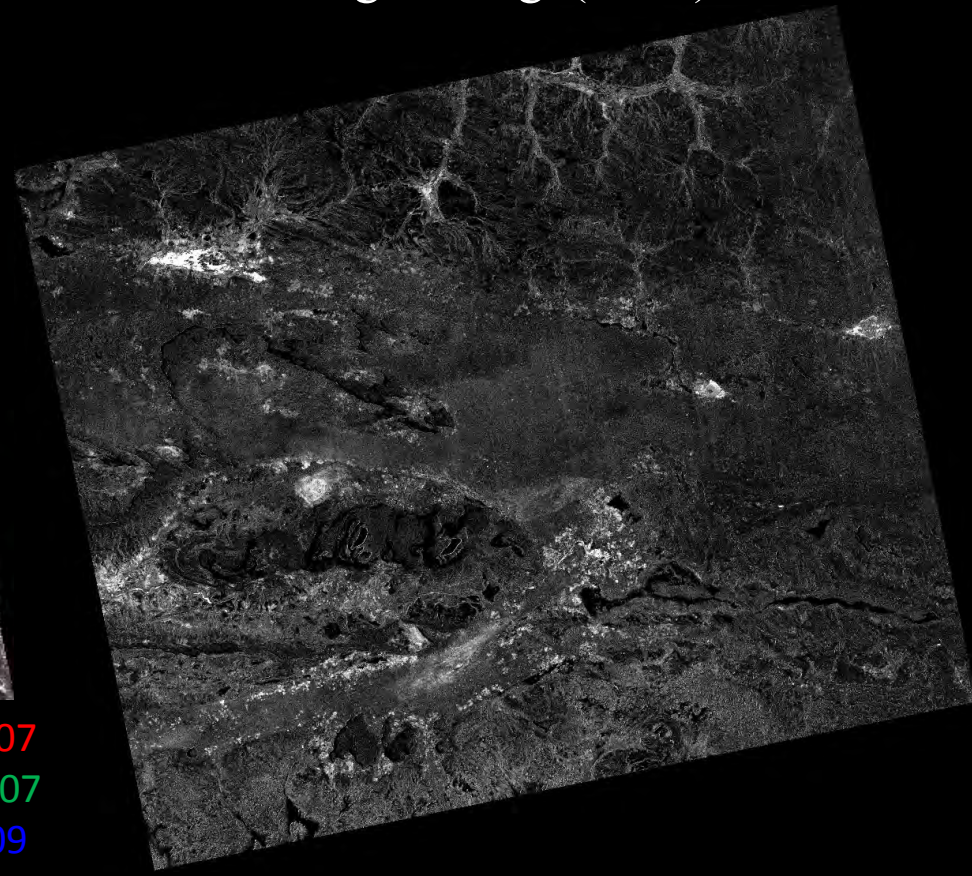
Change detection in a radar time series of 12 PALSAR images Jan. 2007 – apr. 2009

Color composite image



17 Jan. 2007
20 Oct. 2007
22 Jan. 2009

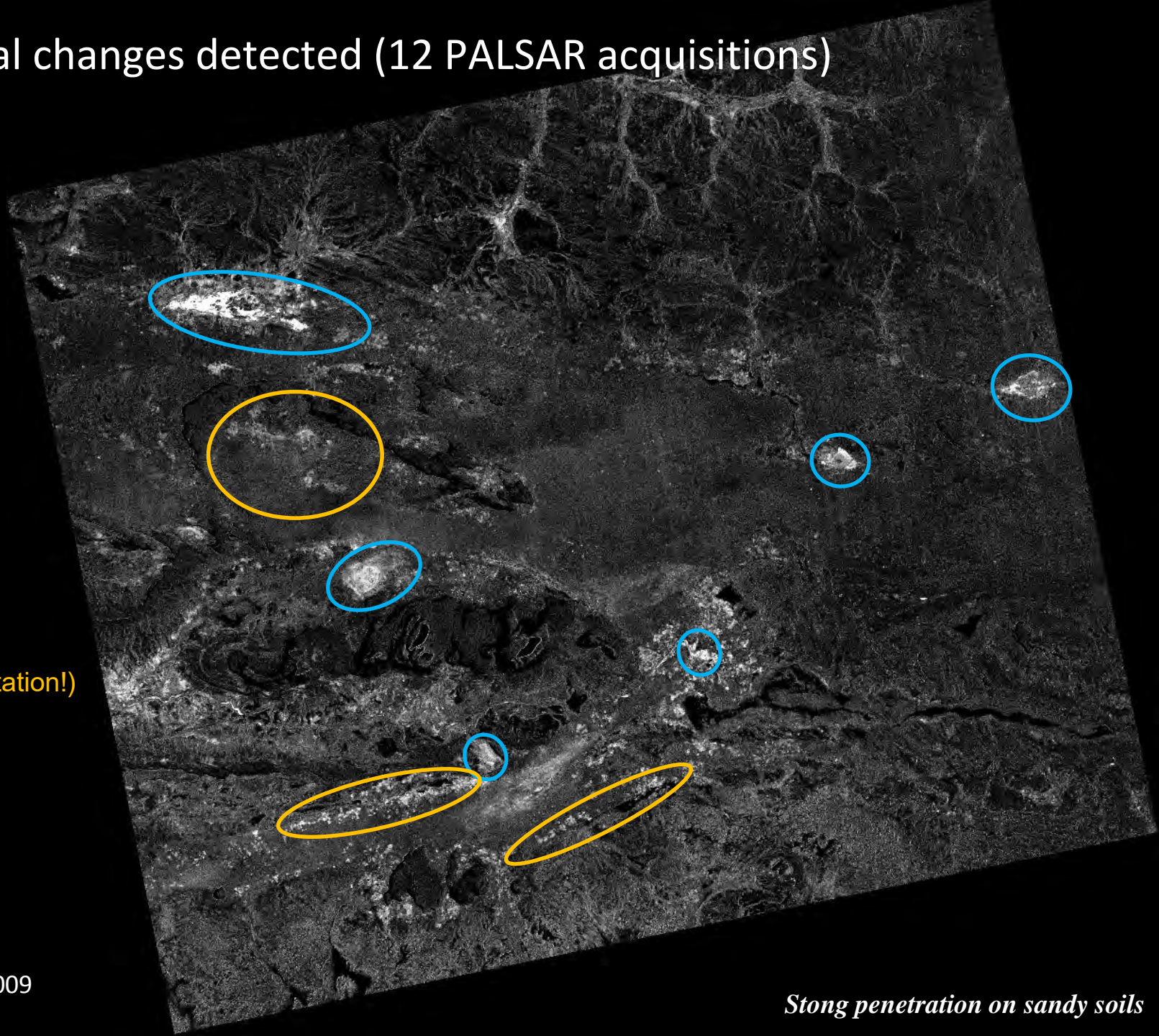
Changes image(HSV)



Jan. 2007 – Apr. 2009

PALSAR Fine Beam
HH polarization

Temporal changes detected (12 PALSAR acquisitions)



ponds

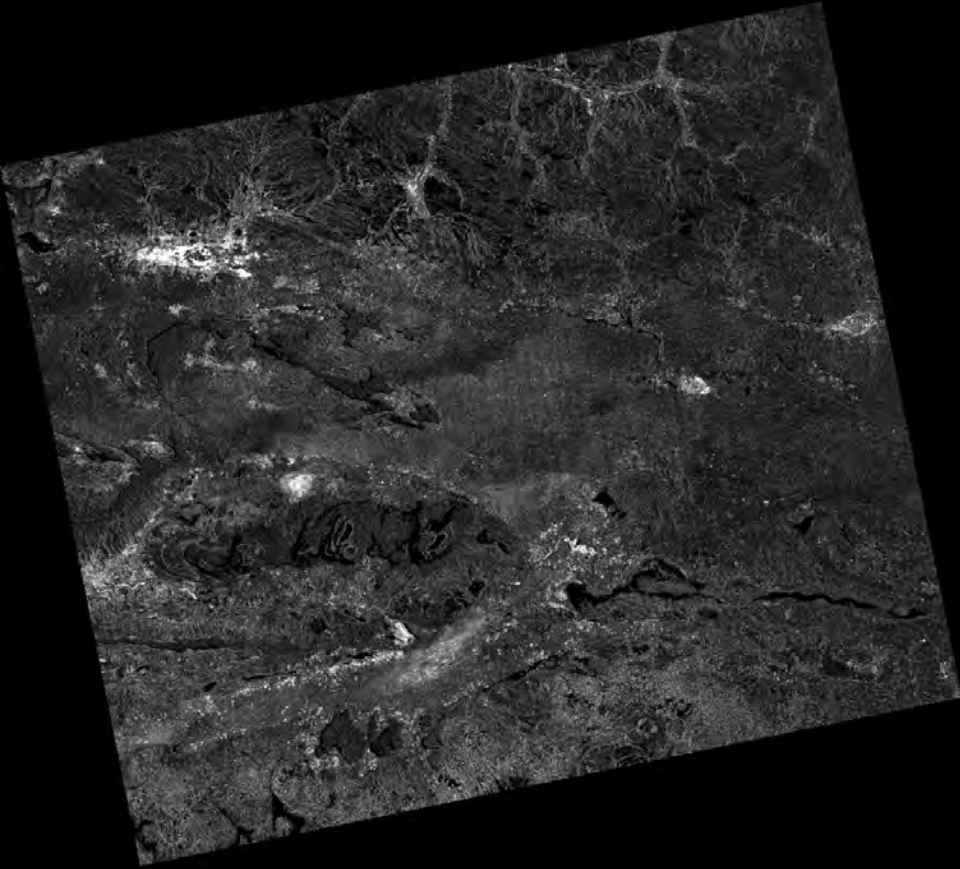
Millet fields
(depend on orientation!)

PALSAR
HH polarisation
Jan. 2007 – Mar. 2009

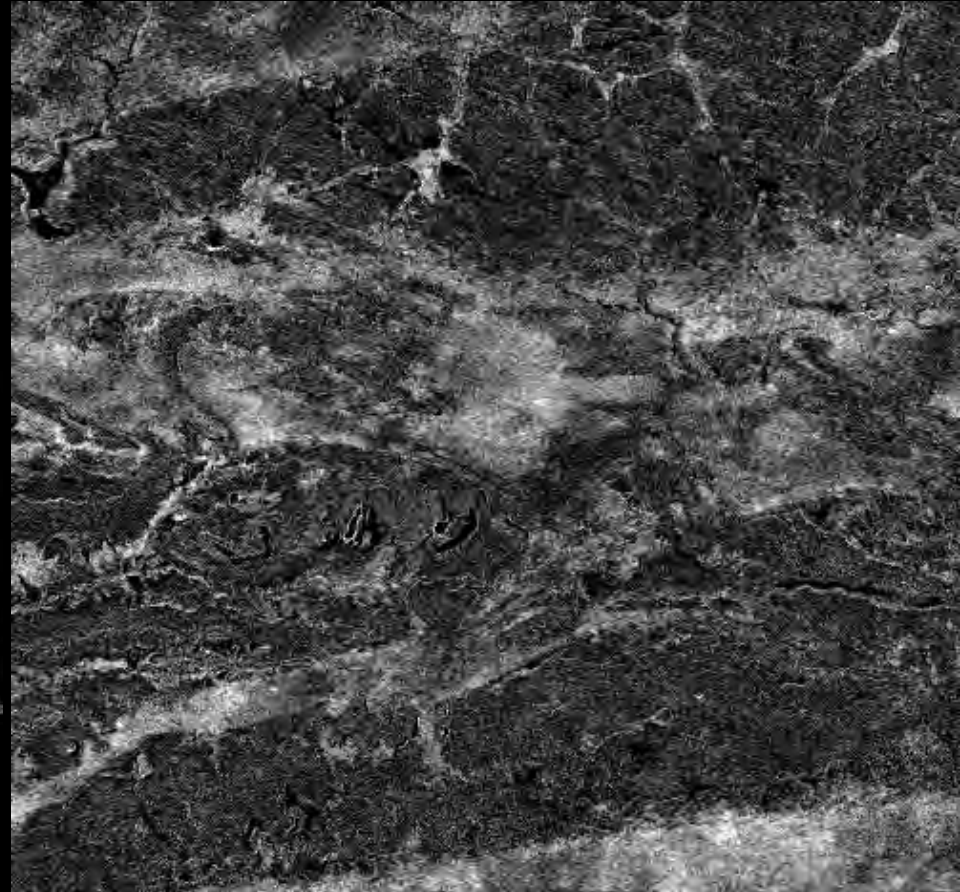
Strong penetration on sandy soils

Changes detection: C band / L band comparison

PALSAR ($\lambda = 24$ cm)

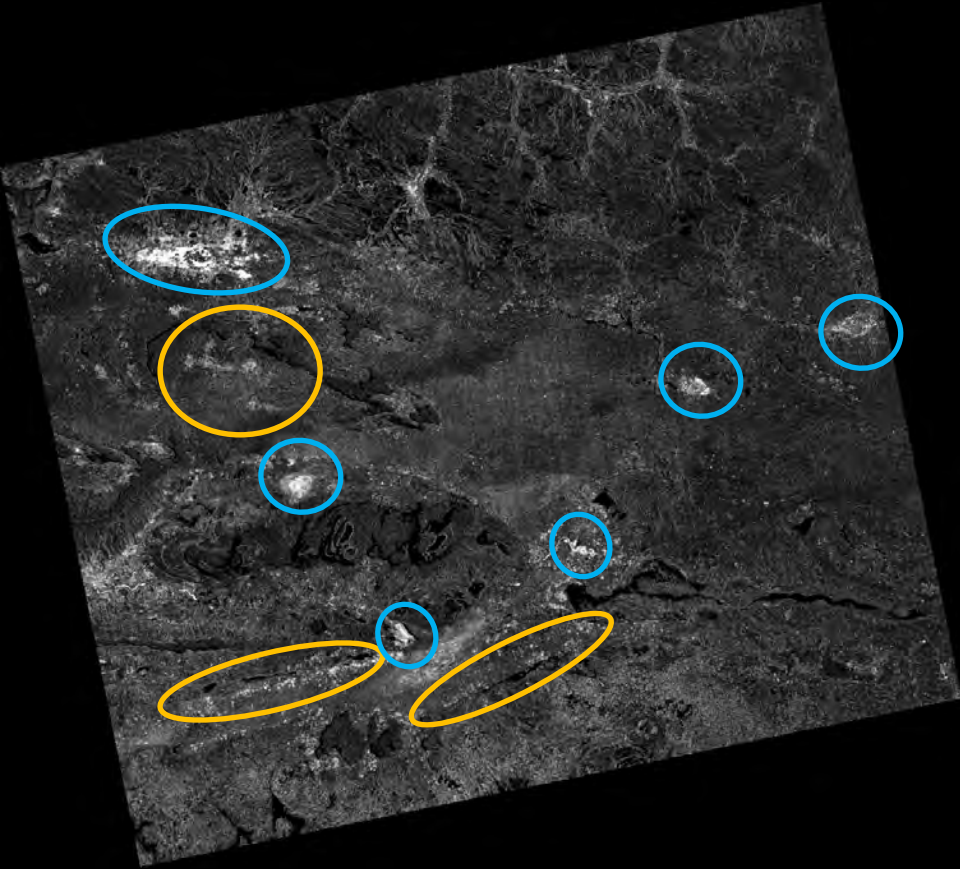


ASAR ($\lambda = 6$ cm)



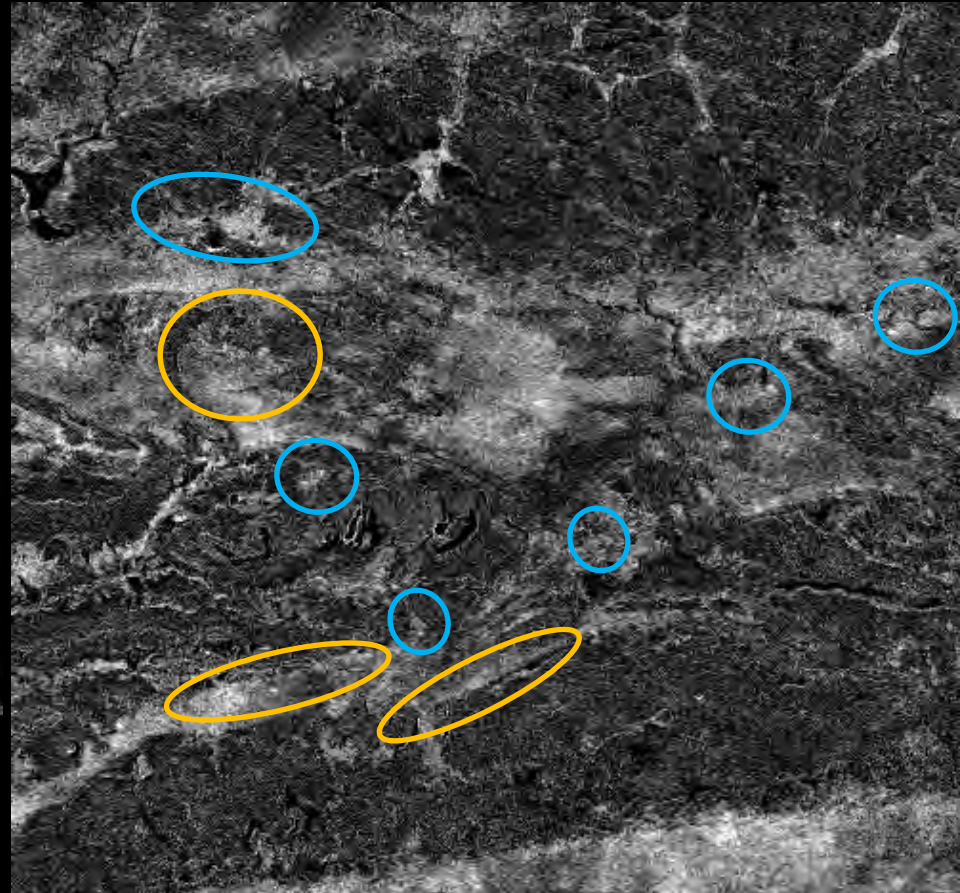
Changes detection: C band / L band comparison

PALSAR ($\lambda = 24$ cm)



Strong penetration on sandy soils
ponds
Millet fields

ASAR ($\lambda = 6$ cm)



Weak penetration on sandy soils
surface states changes
sandy soils, ponds